

ISSN 1023-9855



胸腔醫學

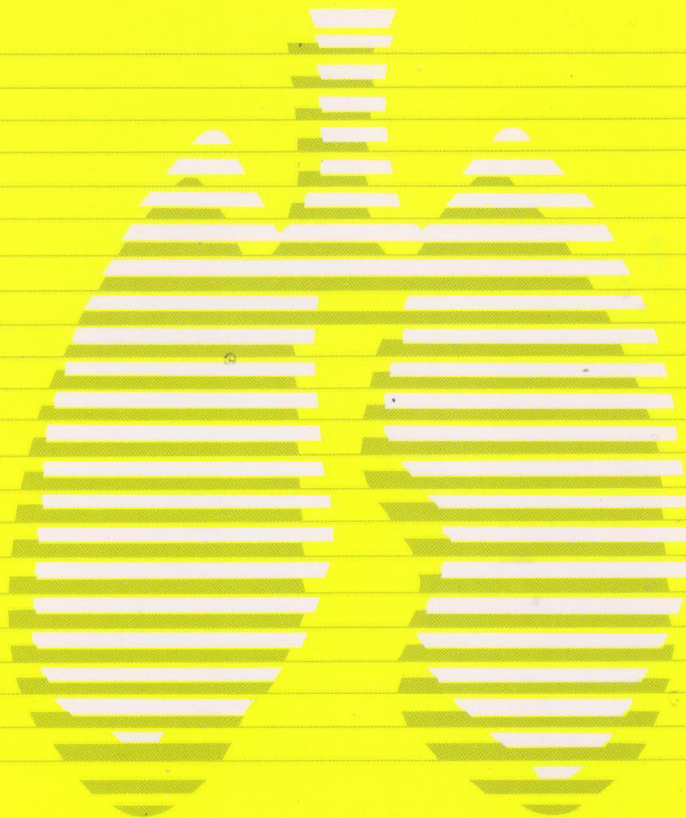
Thoracic Medicine

The Official Journal of Taiwan Society of
Pulmonary and Critical Care Medicine

Vol.23 No.1 Feb. 2008

第二十三卷 第一期

中華民國九十七年二月



台灣胸腔暨重症加護醫學會

台北市中正區仁愛路一段1號

No. 1, Sec. 1, Jen Ai Rd., Taipei, Taiwan, R.O.C.



ISSN 1023-9855



Vol.23 No.1 February 2008

胸腔醫學

Thoracic Medicine

The Official Journal of Taiwan Society
of Pulmonary and Critical Care Medicine

原著

- 骨髓細胞表達的可溶解觸發受體 (sTREM-1)：癌症病人的可能預後因子 1~7
謝國洲，魏裕峰，王誠一，何肇基，余忠仁，楊泮池

病例報告

- 罕見的肝癌肺轉移形式—支氣管內轉移—病例報告 8~13
陳嘉銘，陳家弘，夏德椿，施純明
- 罕見的原發性肺部腫瘤：病例報告 14~18
陳弘興，蔡俊明，彭瑞鵬，錢尚道，許正義
- 罹患阻塞性睡眠呼吸中止症的肥胖糖尿病病患：一病例報告 19~24
黃麗春，江俊松，葉育雯，高尚志，林嘉謨
- 以鈣化性肋膜腔腫瘤為表現的肺吸蟲症：一病例報告 25~30
陳啟信，鄭之勛，黃佩欣，楊泮池
- 肋間肌肉肌內脂肪瘤—病例報告 31~35
林洧呈，張逸良，李元麒
- 原發性食道小細胞癌：二個病例報告 36~41
孫嘉宏，賴信良，彭瑞鵬
- 成人第一型神經纖維瘤併發肺部惡性週邊神經鞘腫瘤轉移——病例報告 42~48
張晟瑜，吳振都，林璟宏，何肇基，楊泮池
- 迷你胸腔鏡手術應用於食道旁支氣管源性囊腫的切除 49~54
李瑞英，李彥龍，李憲斌，周世華，高英隆
- 瀰漫性大 B 細胞淋巴瘤引起的嗜血症候群：病例報告 55~60
陳志雄，鍾焜明，謝俊民，柯獻欽，沈修年，鄭高珍
- 肝臟類上皮性血管內皮瘤以肺部腫塊的不典型表現—病例報告 61~65
游勝耀，林芳杰，曾岐元，吳健樑
- 應用支氣管鏡超音波鑑診斷肺癌與肺結核—病例報告與文獻回顧 66~72
王才郁，郭志熙，陳豪成，吳仁欽，劉劍英



Vol.23 No.1 February 2008

胸腔醫學

Thoracic Medicine

The Official Journal of Taiwan Society
of Pulmonary and Critical Care Medicine

Original Articles

- Soluble Triggering Receptor Expressed on Myeloid Cells 1 (sTREM-1): A Possible Prognostic Factor for Patients with Malignancy 1~7
Kou-Chou Hsieh, Yu-Feng Wei, Cheng-Yi Wang, Chao-Chi Ho, Chong-Jen Yu, Pan-Chyr Yang

Case Reports

- An Unusual form of Metastasis of Hepatocellular Carcinoma — Case Report 8~13
Chia-Ming Chen, Chia-Hung Chen, Te-Chun Hsia, Chuen-Ming Shih
- Primary Lymphoepithelioma-like Carcinoma of the Lung: A Case Report 14~18
Hung-Hsing Chen, Chun-Ming Tsai, Reury-Perng Perng, Shang-Tao Chien, Jane-Yi Hsu
- Obstructive Sleep Apnea in an Obese Patient with Diabetes Mellitus: A Case Report 19~24
Li-Chun Huang, Jiunn-Song Jiang, Diana Yuwung Yeh, Shang Jyh Kao, Chia-Mo Lin
- Calcified Pleural Tumor as a Rare Presentation of Paragonimiasis: A Case Report 25~30
Chi-Hsien Chen, Jih-Shuin Jerng, Pei-Shin Huang, Pan-Chyr Yang
- Intramuscular Lipoma Arising in the Intercostal Muscle — A Case Report 31~35
Wei-Cheng Lin, Yih-Leong Chang, Yung-Chie Lee
- Primary Small Cell Carcinoma of the Esophagus: Two Case Reports 36~41
Chia-Hung Sun, Shinn-Liang Lai, Reury-Perng Perng
- Pulmonary Metastatic Malignant Peripheral Nerve Sheath Tumor in an Adult Patient with Neurofibromatosis Type I — A Case Report 42~48
Cheng-Yu Chang, Chen-Tu Wu, Ching-Hung Lin, Chao-Chi Ho, Pan-Chyr Yang
- Needlescopic Video-assisted Thoracic Surgery for Paraesophageal Bronchogenic Cyst 49~54
Jui-Ying Lee, Yen-Lung Lee, Hsien-Pin Li, Shah-Hwa Chou, Eing-Long Kao
- Hemophagocytic Syndrome Associated with Diffuse Large B-Cell Lymphoma: A Case Report 55~60
Chih-Hsiung Chen, Kun-Ming Chung, Jiunn-Min Shieh, Shian-Chin Ko, Hsiu-Nien Shen, Kuo-Chen Cheng
- Atypical Presentation of Hepatic Epithelioid Hemangioendothelioma as a Pulmonary Mass Lesion on Chest Radiograph: A Case Report 61~65
Sheng-Yao Yu, Fung-J Lin, Chi-Yuan Tzen, Chien-Liang Wu
- Endobronchial Ultrasonography (EBUS) to Differentiate Tuberculoma from Lung Cancer — A Case Report and Literature Review 66~72
Tsai-Yu Wang, Chih-Hsi Kuo, Hao-Cheng Chen, Ren-Chin Wu, Chien-Ying Liu

Soluble Triggering Receptor Expressed on Myeloid Cells 1 (sTREM-1): A Possible Prognostic Factor for Patients with Malignancy

Kou-Chou Hsieh^{*,***}, Yu-Feng Wei^{****}, Cheng-Yi Wang^{*,*****}, Chao-Chi Ho^{*,**},
Chong-Jen Yu^{*}, Pan-Chyr Yang^{*}

Background: The concentration of soluble triggering receptor expressed on myeloid cells-1 (sTREM-1) in malignant pleural effusions is higher than that of transudates. As a marker of inflammation, the correlation of sTREM-1 in serum and pleural effusion is not known. We were interested in the relationship between the prognosis and sTREM-1 in malignant patients.

Methods: We performed a prospective observational study. A total of 17 patients with malignancy were enrolled. The sTREM-1 concentration in serum and pleural effusion was measured using a sandwich enzyme-linked immunosorbent assay. The correlation between serum and pleural effusions was analyzed by nonparametric correlation analysis. The association between sTREM-1 and patient progression-free survival was assessed using the log-rank test.

Results: The correlation between serum and pleural effusions was good (Spearman's correlation coefficient=0.823, $p < 0.01$). Univariate analysis showed the tendency of a shorter progression-free survival in patients with high sTREM-1 levels in serum (≥ 180 pg/ml) than in patients with low sTREM-1 levels. But this result was not confirmed by multivariate analysis.

Conclusions: The sTREM-1 levels in pleural effusions are correlated with the sTREM-1 levels in the serum of malignant patients. High sTREM-1 levels in the serum of malignant patients might lead to a tendency of poor progression-free survival. (*Thorac Med* 2008; 23: 1-7)

Key words: soluble triggering receptor expressed on myeloid cells, pleural effusion, serum, malignancy

Introduction

The triggering receptor expressed on myeloid cells 1 (TREM-1), a receptor expressed on the surface of neutrophils and a subset of monocytes, was identified as a marker of the acute inflam-

matory response to microbial products [1]. A soluble form of TREM-1 (sTREM-1) is released from the activated phagocytes and can be measured in various body fluids. A higher level of sTREM-1 (> 180 pg/ml) and a progressive decline of sTREM-1 in serum indicates a favorable

Departments of *Internal Medicine and **Emergency Medicine, National Taiwan University Hospital, Taipei, Taiwan. ***Department of Internal Medicine, Lishin Hospital, Taoyuan, Taiwan. ****Department of Internal Medicine, E-Da Hospital, I Shou University, Kaohsiung, Taiwan. *****Department of Internal Medicine, Cardinal Tien Hospital, Fu Jen Catholic University, Taipei, Taiwan

Address reprint requests to: Dr. Chao-Chi Ho, Department of Internal Medicine, National Taiwan University Hospital, No. 7, Chung-Shan South Road, Taipei 100, Taiwan

clinical outcome in patients with sepsis [2].

The serum CRP level has been evaluated as an independent predictor of survival in various malignancies [3-6]. In terminal cancer patients, survival time was significantly shorter in the high CRP group (≥ 2.2 mg/dl) than in the lower CRP group [7].

sTREM-1 is a better marker for sepsis than CRP [8]. However, TREM-1 is not up-regulated in infectious disease only, but also in inflammatory disease such as pancreatitis and gouty arthritis [9-10]. Concentrations of sTREM-1 are also higher in malignant pleural effusions than in transudates [11]. sTREM-1, a marker of inflammatory disease like CRP, may be a predictor of prognosis for patients with malignancy.

In this study, we prospectively collected the pleural effusions and serum from patients with malignancy. We investigated the correlation of sTREM-1 between pleural effusions and serum. We also evaluated the possibility of sTREM-1 as a prognostic factor in malignant patients.

Materials and Methods

From September to December 2005, 17 patients with malignancy who were admitted to National Taiwan University Hospital (NTUH) with clinically significant pleural effusion detected either by chest radiograph or ultrasonography were enrolled in the study. Patients with pleural effusion other than malignancy were excluded from the study.

The following clinical data were collected for each patient: age, sex, diagnosis, stage, survival time, progression-free survival time, underlying diseases, and infection parameters, including white cell blood counts with or without CRP.

After obtaining informed consent from patients or next of kin, pleural effusion and serum

were collected and centrifuged at 4°C, separated into aliquots, and stored at -80°C until the day of assay. Concentrations of sTREM-1 in serum and pleural effusion were determined by a sandwich enzyme-linked immunosorbent assay. In short, 96-well goat anti-mouse IgG coated plates (R&D Systems, Minneapolis, MN, USA) were incubated overnight at room temperature with 400 ng per well mouse anti-human TREM-1 capture antibody (R&D Systems). The plates were then washed with 0.05% Tween 20 in phosphate-buffered saline. Samples and standards were diluted in phosphate-buffered saline containing 20% fetal calf serum and incubated for 2 h. Human recombinant sTREM-1 was used as the standard (R&D Systems). After 3 washes, 40 ng per well biotinylated goat anti-human TREM-1 (R&D Systems) was added for 2 h at room temperature. After three washes, bound sTREM-1 was detected with peroxidase-conjugated streptavidin (R&D Systems) and ortho-phenylenediamine as the substrate. The color reaction was stopped after 10 min with 2 N H₂SO₄, and the absorbance was read at 450 and 560 nm for wavelength correction. All measurements were performed in duplicate and in a blinded fashion.

For statistical analysis, data were expressed as mean \pm SD with range, and in the case of a skewed distribution, a median was used with range. We used a chi-square test for categorical variables and the Fisher's exact test, if appropriate, along with the Student's *t* test for continuous variables. Survival curves were constructed using the Kaplan-Meier method, and the differences assessed using the log-rank test. Nonparametric correlation analysis was done for the correlation between sTREM-1 levels in serum and in pleural effusion. Multivariate analysis was performed with the selected variables (age, sex, white blood count, serum sTREM-1 level). Statistical

analyses were performed with the SPSS-13 computer software program (SPSS, Inc., Chicago, IL). A p value of less than 0.05 was considered statistically significant.

Results

During the 3-month study period, 17 patients, with a mean age of 56.58 (range, 23-85) years old and a male percentage of 47%, were enrolled. Among the 17 patients, 5 had non-small cell lung cancer (29.41%), 2 had colon cancer (11.76%), 2 had endometrial cancer (11.76%), 2 had lymphoma (11.76%), 1 had small-cell lung cancer (5.88%), 1 had thymic carcinoma (5.88%), 1 had gastric cancer (5.88%), 1 had hepatocellular carcinoma (5.88%), 1 had cervical cancer (5.88%), and 1 had sarcoma (5.88%).

Soluble TREM-1 was measured in effusions and serum from all the patients. The sTREM-1 levels in effusions were correlated with the sTREM-1 levels in serum, using the Spearman's correlation coefficient 0.852 (Figure 1).

We artificially divided our patients into 2 groups according to the sTREM-1 levels in serum (Group 1: sTREM-1 > 180 pg/ml, Group 2: sTREM-1 < 180 pg/ml). The mean concentration of sTREM-1 in the pleural effusion in group 1 was 963.02 ± 1075.50 pg/mL, and that in group 2 was 104.59 ± 163.23 pg/mL.

Kaplan-Meier survival analysis of the 2 groups categorized by serum sTREM-1 levels demonstrated a tendency of longer progression-free survival in patients with lower serum sTREM-1 levels ($p = 0.052$ by log-rank test, Figure 2). However, sTREM-1 levels in malignant

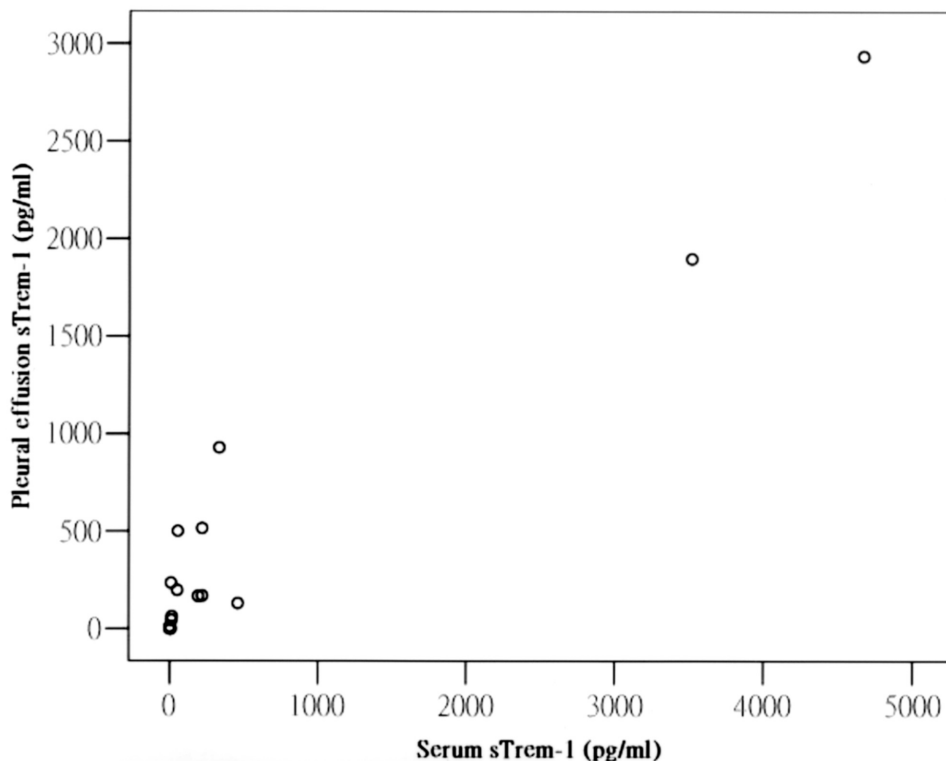


Fig. 1. Simple scatter graph of body fluid and serum sTREM-1 levels. Spearman's correlation coefficient = 0.823, $p < 0.01$

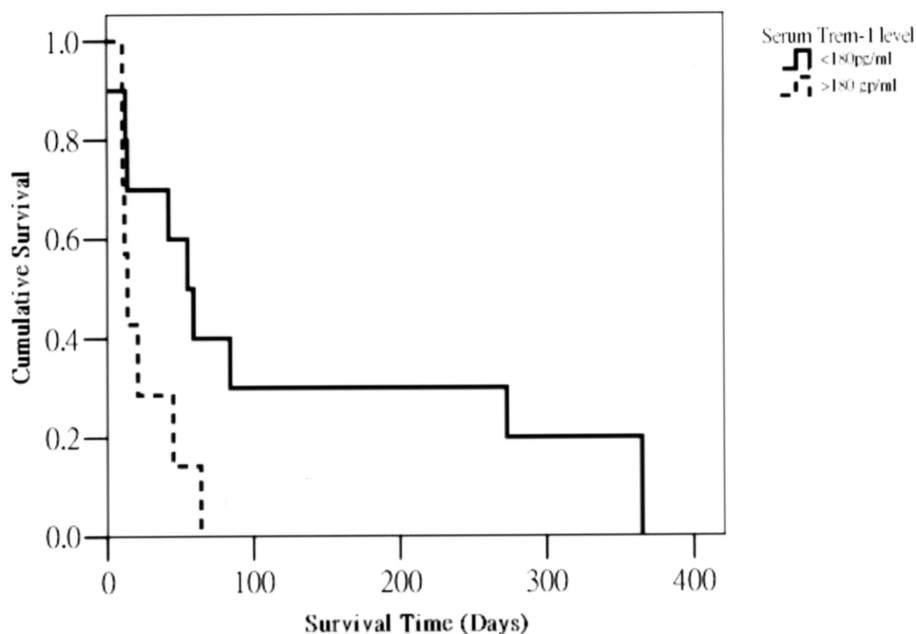


Fig. 2. Progression-free survival curve of high or low serum sTREM-1 levels, $p = 0.052$ by log-rank test

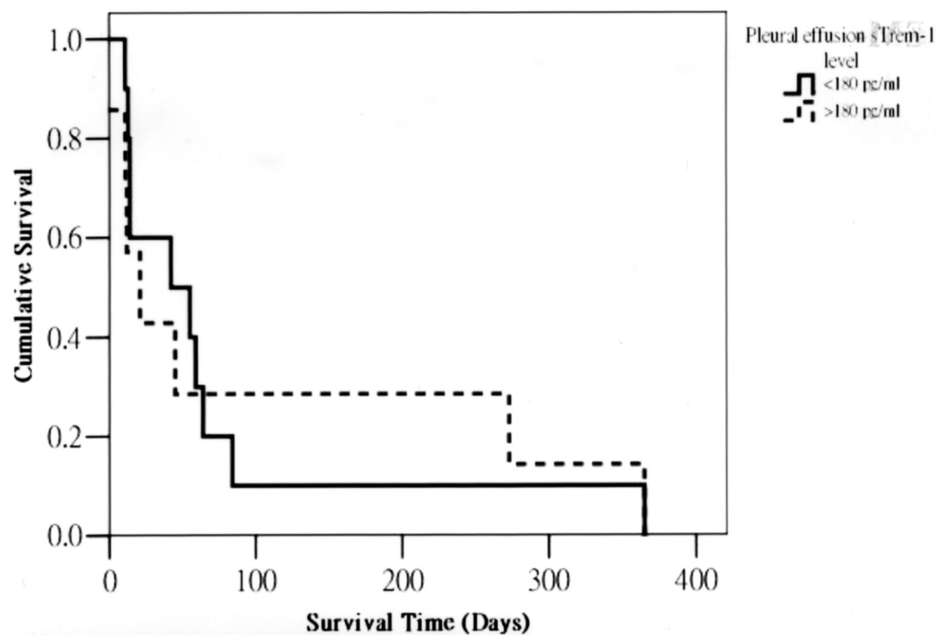


Fig. 3. Progression-free survival curve of high or low sTREM-1 levels in pleural effusion, $p = 0.908$ by the log-rank test

pleural effusions > 180 pg/ml did not predict a poor prognosis (Figure 3). Multivariate analysis failed to demonstrate any independent predictor

for progression-free survival, including sTREM-1 in serum.

Table 1. Characteristics of 17 patients according to serum sTREM-1 levels.

	All patients (n=17)	Serum sTREM-1 > 180 pg/ml (n=7)	Serum sTREM-1 < 180 pg/ml (n=10)	p value
Age (years)	56.00 ± 15.05	46 ± 15.68	63.00 ± 10.31	0.223
Male	(8/17) 47%	(1/7) 14%	(7/10) 70%	0.138
sTREM-1 (serum, pg/ml)	573.54 ± 1347.45	1372.28 ± 1890.95	14.42 ± 20.32	-
sTREM-1 (pleural effusion, pg/ml)	458.06 ± 798.99	963.02 ± 1075.50	104.59 ± 163.23	0.002
PFS	85.24 ± 122.55	25.43 ± 20.89	127.10 ± 147.24	0.001
WBC	13107 ± 11776	13094 ± 7378	13118 ± 15189	0.511
CRP	9.32 ± 8.28	7.61 ± 5.54	11.32 ± 4.45	0.121

*Data are presented as No./total (%) or mean ± SD (No., range).

*PFS (progression-free survival): days before disease progression or mortality.

Discussion

Increased CRP (C reactive protein) levels in patients with colorectal cancer is associated with a more frequent local tumor invasion, fewer curative resections, a higher recurrence rate after surgery, and a higher CEA level [12-13]. The preoperative serum CRP level is an independent and significant indicator predictive of poor prognosis and early recurrence in patients with HCC [14]. CRP elevation is an independent predictor for disease-free survival in patients with RCC [15]. As for CRP, elevated sTREM-1 levels may imply systemic inflammation induced by cancer cells, and thus could be a marker of disease burden.

Sébastien *et al.* demonstrated that higher levels of plasma sTREM-1 (> 180 pg/ml) indicate a favorable clinical evolution in patients with sepsis [2]. In this study, the serum sTREM-1 levels in our patients had a wide range (mean ± SD: 573.54 ± 1347.45 pg/ml, range: 0-4668.87 pg/ml, median: 50.22 pg/ml). No patient had a serum sTREM-1 level between 55 and 180 ng/ml (7 patients had serum sTREM-1 levels > 180 pg/ml and 10 patients had serum sTREM-1 levels

< 55 pg/ml), thus the median was not taken as a cut-off point. We divided our patients into 2 groups by their serum sTREM-1 levels and chose 180 pg/ml as the cut-off point.

This study had significant limitations. First, the number of study subjects was too small and our 17 patients had 10 different malignancies. Second, sTREM-1 is a marker of acute inflammation, and patients with malignancy may be immunocompromised due to malnutrition or chemotherapy. Thus the sTREM-1 levels in this study may be influenced by occult infections. The average CRP level was lower in patients with higher sTREM-1 levels; this discrepancy may be related to the small sample size and different malignancies.

Elevated serum sTREM-1 levels were associated with the tendency toward a shorter progression-free survival in patients with malignancy. The sTREM-1 levels in the pleural effusion were positively correlated with those in the serum. Further study with more cases is necessary to clarify the role of sTREM-1 in patients with malignancy.

Table 2. Multivariate regression

Variables	Regression Coefficient (s)	SE	Odds ratio (95% confidence interval)	<i>p</i> value
Sex (male)	-0.390	0.814	0.677 (0.137-3.336)	0.385
Age	-0.534	0.44	0.586 (0.247-1.389)	0.225
WBC	0.543	0.332	1.721 (0.897-3.302)	0.405
Serum sTrem-1	-0.358	0.413	0.699 (0.311-1.569)	0.785

References

1. Bouchon A, Facchetti F, Weigand MA, *et al.* TREM-1 amplifies inflammation and is a crucial mediator of septic shock. *Nature* 2001; 410: 1103-7.
2. Gibot S, Cravoisy A, Kolopp-Sarda M-N. Time-course of sTREM (soluble triggering receptor expressed on myeloid cells)-1, procalcitonin, and C-reactive protein plasma concentrations during sepsis. *Crit Care Med* 2005; 33:792-6.
3. Falconer JS, Fearon KC, Ross JA, *et al.* Acute-phase protein response and survival duration of patients with pancreatic cancer. *Cancer* 1995; 75: 2077-82.
4. Nozoe T, Matsumata T, Kitamura M, *et al.* Significance of preoperative elevation of serum C-reactive protein as an indicator for prognosis in colorectal cancer. *Am J Surg* 1998; 176: 335-8.
5. Nozoe T, Saeki H, Sugimachi K. Significance of preoperative elevation of serum C-reactive protein as an indicator of prognosis in esophageal carcinoma. *Am J Surg* 2001; 182: 197-201.
6. Kroschinsky F, Weise M, Illmer T, *et al.* Outcome and prognostic features of intensive care unit treatment in patients with hematological malignancies. *Intensive Care Med* 2002; 28: 1294-300.
7. Suh SY, Ahn HY. A prospective study on C-reactive protein as a prognostic factor for survival time of terminally ill cancer patients. *Support Care Cancer* 2007 Jan; 613-20. Epub ahead of print. DOI: 10.1007/s00520-006-0208-5
8. Gibot S, Kolopp-Sarda MN, Bene MC, *et al.* Plasma level of a triggering receptor expressed on myeloid cells-1: its diagnostic accuracy in patients with suspected sepsis. *Ann Intern Med* 2004; 141: 9-15.
9. Wang DY, Qin RY. Expression of TREM-1 mRNA in acute pancreatitis. *World J Gastroenterol* 2004; 10(18): 2744-6.
10. Akahoshi T, Murakami Y, Kitasato Y. Recent advances in crystal-induced acute inflammation. *Current Opinion in Rheumatology* 2007; 19: 146-50.
11. Liu C, Hsieh W, Wu C, *et al.* Triggering receptor expressed on myeloid cells-1 in pleural effusions: A marker of inflammatory disease. *Respiratory Medicine* 2007 May; 101(5): 903-9.
12. Wigmore SJ, McMahon AJ, Sturgeon CM, *et al.* Acute-phase protein response, survival and tumour recurrence in patients with colorectal cancer. *Br J Surg* 2001; 88: 255-60.
13. McMillan DC, Wotherspoon HA, Fearon KC, *et al.* A prospective study of tumor recurrence and the acute-phase response after apparently curative colorectal cancer surgery. *Am J Surg* 1995; 170: 319-22.
14. Hashimoto K, Ikeda Y, Korenaga D, *et al.* The impact of preoperative serum C-reactive protein on the prognosis of patients with hepatocellular carcinoma. *Cancer* 2005; 103: 1856-64.
15. Ito K, Asano T. Impact of thrombocytosis and C-reactive protein elevation on the prognosis for patients with renal cell carcinoma. *International Journal of Urology* 2006; 13: 1365-70.

骨髓細胞表達的可溶解觸發受體（sTREM-1）： 癌症病人的可能預後因子

謝國洲*,*** 魏裕峰**** 王誠一*,***** 何肇基*,** 余忠仁* 楊泮池*

背景：在惡性肋膜積液中，骨髓細胞表達的可溶解觸發受體（sTREM-1）的濃度，較滲出性肋膜積液高。作為發炎反應的指標，血清中與肋膜積液中的 sTREM-1 濃度的相關性還是未知我們同時也對 sTREM-1 濃度與癌症病人預後的關係感到興趣。

方法：這是一個前瞻性的觀察研究，總共有 17 位癌症患者為研究對象。我們利用酵素連結免疫吸附分析的方法測出肋膜積液與血清中 sTREM-1 的濃度。統計上則是利用 *Nonparametric correlation analysis* 來分析肋膜積液與血清中 sTREM-1 濃度的相關性。sTREM-1 濃度與病人的 progression-free survival 的相關性則使用 log-rank test 來分析。

結果：肋膜積液與血清中 sTREM-1 濃度是高度正相關性（Spearman's correlation coefficient=0.823, $p < 0.01$ ）。單變數分析顯示血清中 sTREM-1 濃度較高（ ≥ 180 pg/ml）的病人傾向有較短的 progression-free survival。但多變數分析並未證實此結果。

結論：癌症病人的肋膜積液中 sTREM-1 濃度正相關於血清中 sTREM-1 濃度。血清中 sTREM-1 濃度較高的癌症患者有 progression-free survival 較短的傾向。（*胸腔醫學* 2008; 23: 1-7）

關鍵詞：骨髓細胞表達的可溶解觸發受體（sTREM-1），肋膜積液，血清，癌症

An Unusual form of Metastasis of Hepatocellular Carcinoma — Case Report

Chia-Ming Chen, Chia-Hung Chen, Te-Chun Hsia, Chuen-Ming Shih

Endobronchial metastases (EBM) from extrapulmonary malignant tumors are rare. The most common extrathoracic malignancies associated with EBM are breast, renal and colorectal carcinomas. EBM is defined as bronchoscopically visible lesions histopathologically identical to the primary tumor in patients with extrapulmonary malignancies. Symptoms and radiographic findings are similar to those in primary lung cancer. Therefore, EBM should be differentiated from primary lung cancer histopathologically. Of the many types of extrathoracic tumors capable of EBM, only 2 cases of EBM from hepatocellular carcinoma have been reported in the literature. We report a patient present with right lower lobe collapse and bronchoscopic biopsy-confirmed EBM from hepatocellular carcinoma. (*Thorac Med* 2008; 23: 8-13)

Key words: hepatoma, endobronchial metastasis

Introduction

A variety of malignancies can metastasize to the lung, the hilar and mediastinal lymph nodes, and the pleura [1]. However, endobronchial metastases (EBM) are uncommon. The frequency of EBM varies depending upon the definition, ranging from 2-50% of pulmonary metastases from extra-thoracic neoplasms [2-4]. A variety of tumors have been associated with EBM, including breast, colorectal, renal, ovarian, thyroid, uterine, testicular, head-neck, prostate and adrenal carcinomas, sarcomas, melanomas and plasmacytomas [5-10]. Breast, renal and colorectal carcinomas are the most common primary tumors that metastasize to the lung [2, 11-13].

It is important to make a distinction between EBM and primary lung cancers and benign lesions, as treatment approaches will differ [14-15]. An exact histological diagnosis needs to be established in each patient. Of the many types of extrathoracic tumors capable of EBM, only 2 cases of EBM from hepatocellular carcinoma have been reported in the English literature [12, 17], since hepatocellular carcinoma with lung metastasis usually presents with multiple pulmonary lesions. We herein report a patient present with right lower lobe collapse and bronchoscopic biopsy confirm EBM from hepatocellular carcinoma.

Division of Pulmonary and Critical Care Medicine, China Medical University Hospital, Taichung, Taiwan, R.O.C.
Address reprint requests to: Dr. Chuen-Ming Shih, Department of Internal Medicine, China Medical University Hospital, No. 2, Yude Road, Bei Chiu, Taichung, Taiwan 404, R.O.C.

Case Report

A 53-year-old housewife had been diagnosed with hepatocellular carcinoma about 3 years previously. She has been treated with transcatheter arterial chemoembolism (TACE) 3 times, and a right lung nodule was noted at that time. Bronchoscopic biopsy was negative for malignant cells. Recurrent hepatocellular carcinoma was found about 6 months before this admission. She refused TACE again and was treated with herbal



Fig. 1. Chest plain film showing a right major fissure downward deviation and right lower lobe collapse.

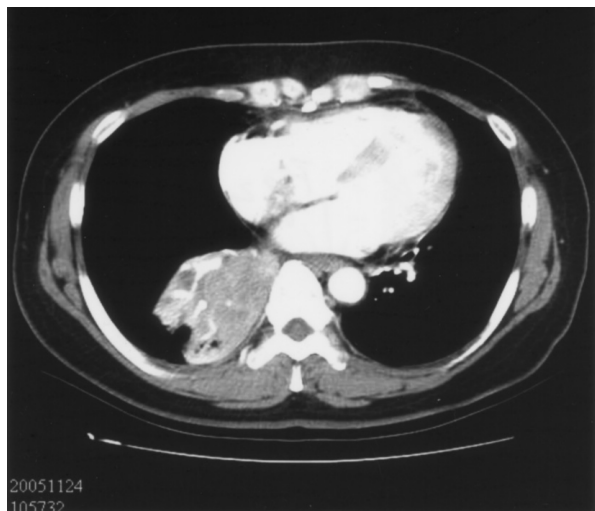


Fig. 2. Chest CT reveals right lower lobe collapse

medicine. Cough was noted for about 1 month before this admission. Wheezing sounds were noted while lying down. Chest radiography revealed right lower lobe collapse (Figure 1). One day prior to admission, hemoptysis of about 100 cc was noted, and she was admitted for further evaluation.

On physical examination at admission, decreased breathing sounds in the right lower lung were noted. Laboratory tests showed no coagulopathy. The PT was 15.28 seconds and the INR was 1.30, APTT was 28.40 seconds, and α -fetoprotein was 864 ng/ml. Complete blood count revealed a hemoglobin value of 13.5 gm/dl and a platelet count value of 51000/ul. Chest radiography showed multiple lung nodules in the right lung. One day later, chest radiography showed right middle and right lower lobe collapse. High resolution computer tomography (HRCT) of the chest showed a focal lesion in right lower lobe with occlusion of right lower lobe bronchi (Figure 2). A small nodule was in the lateral segment of the right middle lobe.

Fibrobronchoscopy revealed a right lower lobe inlet tumor with total occlusion (Figure 3). Broncho-scopic alveolar lavage and brushing



Fig. 3. Bronchoscopy reveals a right lower lobe inlet tumor with total occlusion.

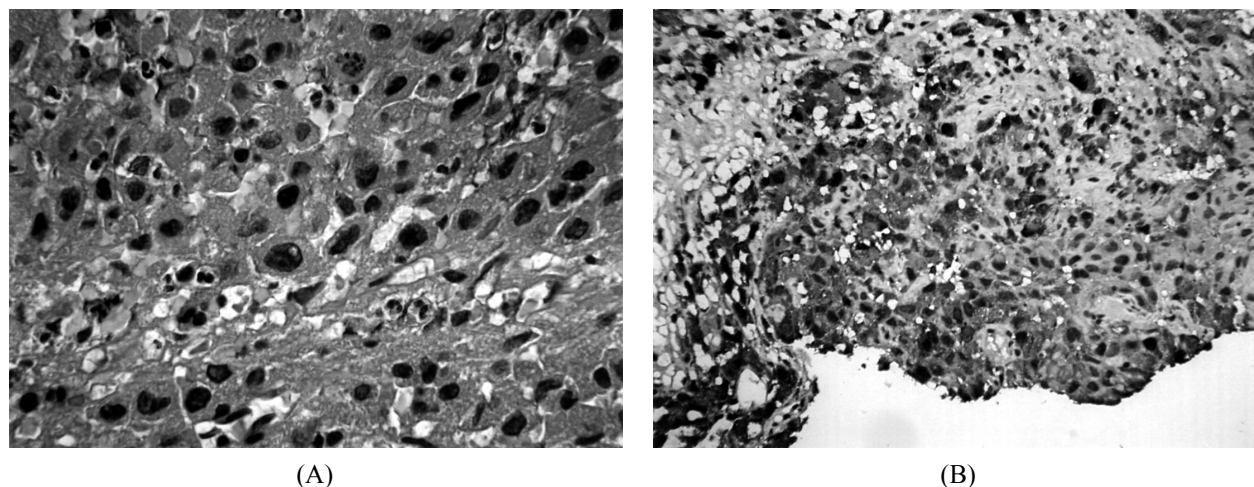


Fig. 4. A) Specimen of the right lower lobe bronchus reveals non-small cell carcinoma [H&E stain X400]. B) Immunohistochemical study reveals tumor cells positive for CK8 [200 X].

cytology were positive for malignancy, favoring adenocarcinoma. However, bronchoscopic biopsy revealed a non-small cell carcinoma of the right lower bronchus (Figure 4A). Pleomorphic tumor cells arranged in solid sheets with distinct nucleoli were seen. The immunohistochemical study was negative for thyroid transcription factor-1 (TTF-1), and squamous cell carcinoma was more likely. Because of the worsening dyspnea and right lower lung consolidation revealed on chest radiography, an endobronchial tumor causing the right lower lobe collapse was suspected. Endobronchial electrocautery with total clearance of the airway tumor was performed. Pathology showed the picture of a poorly differentiated carcinoma of the lung comprised of a nesting, trabecular or sinusoid arrangement of tumor cells infiltrating in the lung parenchyma. The tumor cells contained round to oval hyperchromatic nuclei, and eosinophilic to pale staining cytoplasm; tumor necrosis was also noted. Immunohistochemically, the tumor cells were reactive for cytokeratin 8 (Figure 4B) and alfa-fetal protein, and non-reactive for CEA, TTF-1, or 34 beta E12. The

clinical history, histopathologic picture, and the immunoprofiles were compatible with metastatic hepatocellular carcinoma. The patient developed acute respiratory failure later due to nosocomial pneumonia with right empyema, and received endotracheal tube intubation with ventilator support. After antibiotics treatment and tube thoracostomy, her condition stabilized. She was extubated about 40 days after admission and later discharged.

Discussion

EBM defines a bronchoscopically visible nonpulmonary neoplasm metastasizing to the bronchus histologically identical to non-pulmonary cancer. EBM are rare in comparison with parenchymal deposits, and account for 2% of deaths from solid neoplasms. The incidence of EBM is increasing because of the regular use of fiberoptic bronchoscopy and the longer survival of cancer patients. The tumors that cause EBM include breast, colorectal, renal, ovarian, thyroid, uterine, testicular, nasopharynx, prostate and

adrenal carcinomas; sarcomas; melanomas and plasmacytomas. Kidney, colon, and breast cancer and melanoma account for 67% of the cases. EBM of hepatocellular carcinoma is rare. To our knowledge, only 2 cases have been reported in the past two decades [12, 17].

Various possible modes of development of EBM have been studied [1, 4], and include: type I, direct metastasis to the bronchus; type II, bronchial invasion by a parenchymal lesion; type III, bronchial invasion by mediastinal or hilar lymph node metastasis; and type IV, peripheral lesions extending along the proximal bronchus [8]. The EBM in our report seems to have been type II or IV, because there was a small nodule in the lateral segment of the right middle lobe.

The presenting manifestations of EBM are similar to those of centrally located primary bronchogenic carcinoma with cough, hemoptysis, atelectasis and post-obstructive pneumonia, though 50-60% of the patients are asymptomatic. Dyspnea and wheezing are far less common. Chest radiographic findings may be normal or show atelectasis, nodules, a hilar mass and mediastinal adenopathy.

EBM are, on average, diagnosed about 4 years after the diagnosis of primary neoplastic disease, which is a relatively long lead-time, given the average time to progression in these solid tumors [12]. However, there is no data available about how long after the diagnosis of hepatocellular carcinomas EBM will develop. Extra-thoracic malignancy usually antecedes EBM but can also be diagnosed simultaneously. Atelectasis or obstructive pneumonia, pulmonary nodular mass with hilar lymph node swelling or mediastinal mass were observed on the chest X-ray of patients with EBM [19-20]. Besides the main metastatic lesion, multiple bilateral or unilateral pulmonary nodules, diffuse interstitial infiltration,

and pleural effusion can occur concurrently in patients with EBM [13-16, 18]. A normal CXR is extremely rare [12]. Most of the patients had radiographic signs of hematogenous or lymphatic spread and no one had a normal CXR. Pulmonary parenchymal metastases usually occurred in the lower lobes. In the report of Kiryu *et al.* [13], there was a predominance of right-sided lesions, and the reason for this was uncertain.

The diagnosis of EBM is readily evaluated by bronchoscope and biopsy [21]. However, sometimes it is not easy to distinguish metastasis from primary lung cancer. Immunohistochemical staining can help in the diagnosis.

References

1. Shepherd MP. Thoracic metastases. *Thorax* 1982; 37: 366-70.
2. Braman SS, Whitcomb ME. Endobronchial metastasis. *Arch Intern Med* 1975; 135: 543-7.
3. King DS, Castleman B. Bronchial involvement in metastatic pulmonary malignancy. *J Thorac Surg* 1943; 12: 305-15.
4. Shepherd MP. Endobronchial metastatic disease. *Thorax* 1982; 37: 362-5.
5. DeBeer RA, Garcia RL, Alexander SC. Endobronchial metastasis from cancer of the breast. *Chest* 1978; 73: 94-6.
6. Noy S, Michowitz M, Lazebnik N, *et al.* Endobronchial metastasis of renal cell carcinoma. *J Surg Oncol* 1986; 31: 268-70.
7. Berg HK, Petrelli NJ, Herrera L, *et al.* Endobronchial metastasis from colorectal carcinoma. *Dis Colon Rectum* 1984; 27: 745-8.
8. Mateo F, Serur E, Smith PR. Bronchial metastases from ovarian carcinoma. Report of a case and review of the literature. *Gynecol Oncol* 1992; 46: 235-8.
9. Lee DW, Ro JY, Sahin AA, *et al.* Mucinous adenocarcinoma of the prostate with endobronchial metastasis. *Am J Clin Pathol* 1990; 94: 641-5.
10. Cicero R, Navarro F, Carrera E, *et al.* Endobronchial metastasis. Experience in two tertiary care hospitals. *J Bronchol* 2001; 8: 84-7.
11. Heitmiller RF, Marasco WJ, Hruban RH, *et al.* Endobron-

- chial metastasis. *J Thorac Cardiovasc Surg* 1993; 106: 537-42.
12. Salud A, Porcel JM, Rovirosa A, *et al.* Endobronchial metastatic disease: analysis of 32 cases. *J Surg Oncol* 1996; 62: 249-52.
13. Kiryu T, Hoshi H, Matsui E, *et al.* Endotracheal/endobronchial metastases: clinicopathologic study with special reference to developmental modes. *Chest* 2001; 119: 768-75.
14. Bourke SJ, Henderson AF, Stevenson RD, *et al.* Endobronchial metastases simulating primary carcinoma of the lung. *Respir Med* 1989; 83: 151-2.
15. Sorensen JB. Endobronchial metastases from extrapulmonary solid tumours. *Acta Oncol* 2004; 43: 73-9.
16. Di Giorgio A, Mingazzini P, Sammartino P, *et al.* Host defense and survival in patients with lung carcinoma. *Cancer* 2000; 89: 2038-45.
17. Lee KY, Ryu SJ, Joo M. Endobronchial metastasis of hepatocellular carcinoma. *Yonsei Med J* 2003; 44: 544-7.
18. Baumgartner WA, Mark JB. Metastatic malignancies from distant sites to the tracheobronchial tree. *J Thorac Cardiovasc Surg* 1980; 79: 499-503.
19. Katsimbri PP, Bamias AT, Froudarakis ME, *et al.* Endobronchial metastases secondary to solid tumors: report of eight cases and review of the literature. *Lung Cancer* 2000; 28: 163-70.
20. Ikezoe J, Johkoh T, Takeuchi N, *et al.* CT findings of endobronchial metastasis. *Acta Radiol* 1991; 32: 455-60.
21. Diaz G, Jimenez D, Dominguez-Reboiras S, *et al.* Yield of bronchoscopy in the diagnosis of neoplasm metastatic to lung. *Respir Med* 2003; 97: 27-9.

罕見的肝癌肺轉移形式—支氣管內轉移—病例報告

陳嘉銘 陳家弘 夏德椿 施純明

支氣管內轉移定義為在內視鏡下可見的支氣管內病灶，最終診斷為肺外惡性腫瘤。由於從症狀及影像上不易與原發性肺腫瘤區分，因此常常需要病理組織學來鑑別。肺外腫瘤以支氣管內轉移來表現的相當罕見，造成支氣管內轉移的肺外腫瘤中以乳癌，腎細胞癌及大腸直腸癌最為常見。肝癌合併支氣管內轉移則非常少見，在文獻中，只有兩個病例。我們將報告一個 53 歲女性肝癌患者，因咳血求診，在胸部 X 光片上呈現右下肺葉萎陷，經由支氣管鏡做病理切片，確診為肝癌合併支氣管內轉移。(胸腔醫學 2008; 23: 8-13)

關鍵詞：肝癌，支氣管內轉移

Primary Lymphoepithelioma-like Carcinoma of the Lung: A Case Report

Hung-Hsing Chen*, Chun-Ming Tsai*, **, Reury-Perng Perng*, **, Shang-Tao Chien***, Jane-Yi Hsu****

A 51-year-old man was found incidentally to have a mass at the lower lobe of the right lung incidentally. He was asymptomatic and was a non-smoker, and his health condition had been good. The chest radiograph showed a mass lesion at the lower lobe of the right lung and subsequent examination favored primary lung cancer. Surgical resection of the tumor was performed and the pathological examination revealed distinct features compatible with lymphoepithelioma-like carcinoma of the lung. In situ hybridization further confirmed the presence of EBER-1 (EBV-encoded small nuclear RNA-1).

Primary lymphoepithelioma-like carcinoma of the lung is a rare pulmonary lung cancer. Prior to 1982, the WHO lung cancer classification did not include this rare entity. Herein we present a rare case of this type of cancer and review the literatures. (*Thorac Med* 2008; 23: 14-18)

Key words: lymphoepithelioma-like carcinoma, Epstein-Barr virus (EBV), primary lung cancer

Introduction

C. Regaud reported a form of nasopharyngeal carcinoma in 1921, which was characterized by undifferentiated neoplastic cells infiltrating with dense lymphocytes, and coined the term "lymphoepithelioma" to describe it [1]. Later, similar tumors were found in a variety of organs, including the thymus [2], parotid gland [3], uterine cervix [4], and skin [5], and the term "lymphoepithelioma-like carcinoma" (LELC) was used. Begin *et al.* reported the first case of lymphoepithelioma-like carcinoma of the lung in a Filipino in 1987, and, based on the immunological

profiles, suggested that Epstein-Barr virus had a role in the pathogenesis [6]. After Begin's report, Butler and Pittaluga also reported cases of primary LELC of the lung and demonstrated the presence of Epstein-Barr virus (EBV) DNA in the tumor cells [7-8]. Until now, there has been about 150 case reports worldwide, and about two-thirds are from southern China, Taiwan and Hong Kong [9]. Herein, we present a case of this rare primary lung cancer and review the literature.

Case Report

A 51-year-old man was found incidentally

*Department of Chest Medicine, Taipei Veterans General Hospital, **Department of Internal Medicine, School of Medicine, National Yang Ming University, Taipei, Taiwan, ***Department of Pathology, Kaohsiung Armed Forces General Hospital, ****Division of Chest Surgery, Kaohsiung Armed Forces General Hospital
Address reprint requests to: Dr. Chun-Ming Tsai, Department of Chest Medicine, Taipei Veterans General Hospital, 201, Section 2, Shih-Pai Road, Taipei 112, Taiwan

to have a mass at the lower lobe of the right lung. The man had been well, except a 10-year history of mild type 2 diabetes mellitus. During a physical check-up, the physical examination disclosed no abnormalities, but chest radiography revealed a mass lesion at the lower lobe of the right lung (Figure 1). He was a non-smoker and asymptomatic. Computed tomography of the chest showed an irregular mass, measuring 3.2 x 2.3 x 2.8 cm in size (Figure 2), with an enlarged lymph node at the right hilum. The whole body bone scan, abdominal computed tomography (CT) scanning, magnetic resonance imaging of the brain and positron emission tomography scanning of the whole body were all negative for distant metastasis. Serum CA-125 was elevated about 4-fold (120 U/ml, N: < 35). Other tumor markers, including CEA and CA-199 were normal. The patient received a lobectomy of the right lower



Fig. 1. The preoperative standing chest radiograph showing a mass lesion at the lower lobe of the right lung.

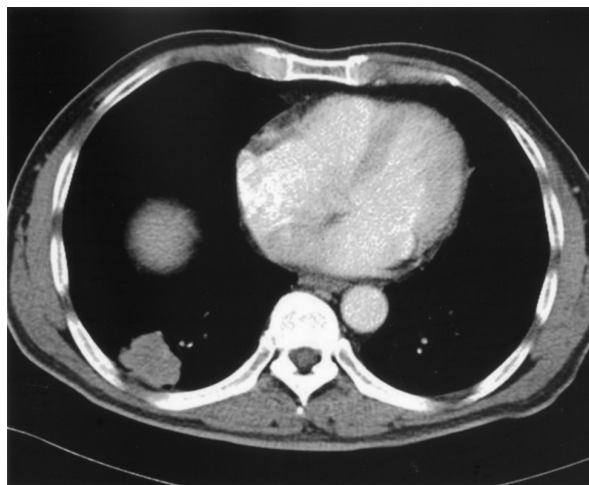


Fig. 2. Contrast-enhanced chest CT scanning shows a mass lesion with soft tissue density and irregular margin. Adjacent pleural thickening was also noted.

lobe and radical lymph node dissection in Jan. 2007. The pathological examination found large undifferentiated neoplastic cells with a syncytial growth pattern, and prominent and large nucleoli, densely infiltrated with lymphocytes, which suggested LELC of the lung. In situ hybridization (PanPath B.V., standard protocol) demonstrated the presence of EBER-1 (EBV-encoded small nuclear RNA-1) in the nuclei of the tumor cells and confirmed the diagnosis (Figure 3). The serology test for precedent EBV infection was positive. The pathological staging was T2N1M0, stage IIB, with positive hilar lymphadenopathy. Adjuvant chemoradiotherapy was administered. Until now, he is receiving regular follow-up without evidence of relapse or disease in progression.

Discussion

Primary LELC of the lung is different from other primary lung cancers with distinct clinicopathological features. Currently, there are only about 150 case reports worldwide and most were from southern China, Taiwan and Hong Kong [9].

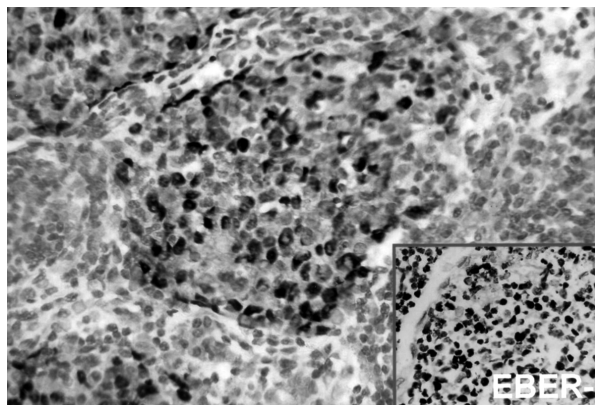


Fig. 3. In situ hybridization shows clusters of neoplastic cells, positive for EBV-encoded small nuclear RNA-1 (EBER-1) and densely infiltrated with lymphocytes.

According to the reports from China [10], primary LELC of the lung represented 0.9% of primary lung cancers. The mean age at diagnosis has been reported to be 10 years younger than that for other primary lung cancers. The stage at diagnosis is earlier and the prognosis is better. Most affected patients are non-smokers. There is no sex predilection. The pathological features are tumor cells growing in anastomosing clusters or diffuse sheets with vesicular chromatin, distinct nucleoli, occasional spindle cell growth, and moderate to heavy infiltration of lymphocytes. Studies by John and Alexandra regarded it as undifferentiated or poorly differentiated squamous cell carcinoma [17-18]. A major differential diagnosis is lymphoma, which can be differentiated by staining with antibody to cytokeratin [18]. The tumor cells are positive for cytokeratin, but the infiltrative lymphocytes are negative. The predominant infiltrative lymphocytes can be CD3-positive T cells or CD20-positive B cells [11-14], and their role can be considered as a local immunological response to neoplasm and virus. Despite these distinctive clinicopathological features, the image findings are nonspecific and cannot be used to differentiate it from other primary lung cancers.

The most common radiographic features are a solitary peripheral nodule or mass, slight contrast-enhancement and occasional central necrosis [15].

EBV has been implicated in the pathogenesis of primary LELC of the lung. In addition to serological evidence, EBER-1 can be directly detected in these neoplastic cells using in situ hybridization [16]. In addition, the finding of a single episomal form of EBV in the tumor suggested that EBV infection occurred before clonal expansion [8]. Therefore, like nasopharyngeal carcinoma, EBV infection may incite neoplastic change in the respiratory epithelium, and then the tumor is secondarily and heavily infiltrated with lymphocytes due to an immunological reaction. However, the strong causative relationship between EBV infection and primary LELC of the lung exists only among Asians. Also, evidence of precedent EBV infection cannot be found in some LELC outside the lung [12-14]. The reasons for these differences still need to be explored.

Surgical resection with or without radiotherapy remains the choice of treatment for early stage tumor (stage I/II). According to the reports of Han, *et al.*, 2-year and 5-year survival rates with stage I disease were 75% and 37.5%, respectively [19]. As for late-stage tumor, multimodality treatment has been suggested. The prognosis is generally better than that of other primary lung cancers.

In conclusion, primary LELC of the lung is regarded as a kind of rare primary lung cancer which could be caused by precedent EBV infection. Smoking is not an important risk factor. Although this is a rare disease, it should be carefully differentiated from lymphoma and metastatic nasopharyngeal carcinoma, especially in Asians. Early diagnosis and surgical intervention offer the best outcome.

References

1. Regaud C, Reverchon L. Sur un cas d'epithelioma epidermoide developpe' dans le massif maxillaire superieur, etendu aux teguments de la face, aux cavites bussale, nasale et orbitaire, ainsiqu' aux ganglions du cou, quero par le curietherapie. *Rev Laryngol* 1921; 42: 369-78.
2. Wick MR, Scheithauer BW, Weiland LH, *et al.* Primary thymic carcinomas. *Am J Surg Pathol* 1982; 6: 613-30.
3. Nagao K, Matsuzaki O, Saiga H, *et al.* A histopathologic study of benign and malignant lymphoepithelial lesions of the parotid gland. *Cancer* 1983; 52: 1044-52.
4. Mills SE, Austin MB, Randall ME. Lymphoepithelioma-like carcinoma of the uterine cervix: a distinctive undifferentiated carcinoma with inflammatory stroma. *Am J Surg Pathol* 1985: 883-9.
5. Swanson SA, Cooper PH, Mills SE, *et al.* Lymphoepithelioma-like carcinoma of the skin. *Mod Pathol* 1988: 359-65.
6. Begin LR, Eskandari J, Joncas J, *et al.* Epstein-Barr virus-related lymphoepithelioma-like carcinoma of the lung. *J Surg Oncol* 1987: 280-3.
7. Butler AE, Colby TV, Weiss L, *et al.* Lymphoepithelioma-like carcinoma of the lung. *Am J Surg Pathol* 1989: 632-9.
8. Pittaluga S, Wong MP, Chung LP, *et al.* Clonal Epstein-Barr virus in lymphoepithelioma-like carcinoma of the lung. *Am J Surg Pathol* 1993: 678-82.
9. James C. HO, Maria P. Wong, Wah K. LAM. Lymphoepithelioma-like carcinoma of the lung. *Respirology* 2006: 539-45.
10. Han AJ, Xiong M, Zong YS. Association of Epstein-Barr virus with lymphoepithelioma-like carcinoma of the lung in southern China. *Am J Clin Pathol* 2000: 220-6.
11. Hendrik W. Elzevier, Pieter L. Venema, Rene F. Kropman, *et al.* Lymphoepithelioma-like carcinoma of the kidney. *J Urol* 2002; 167: 2127-8.
12. Yuly N. Chalikh, Rosemary Wiczorek, Michael Grasso. Lymphoepithelioma-like carcinoma of the ureter. *J Urol* 1998;1 59: 503-4.
13. W G McCluggage. Lymphoepithelioma-like carcinoma of the vagina. *J Clin Pathol* 2001; 54: 964-5.
14. Kwai-Fong NG, Tse-Ching Chen, Phei-Lang Chang. Lymphoepithelioma-like carcinoma of the ureter. *J Urol* 1999; 161: 1277-8.
15. Joseph M, Hoxworth Douglas K, Hanks Philip A. Lymphoepithelioma-like carcinoma of the lung: radiologic features of an uncommon primary pulmonary neoplasm. *Am J Roentgenol* 2006: 1294-9.
16. Weiss LM, Movahed LA, Butler AE, *et al.* Analysis of lymphoepithelioma and lymphoepithelioma-like carcinomas for Epstein Barr viral genomes by in situ hybridization. *Am J Surg Pathol* 1989; 13: 625-31.
17. John K.C. Chan, Pak-Kwan Hui, William Y. W. Tsang. Primary lymphoepithelioma-like carcinoma of the lung. *Cancer* 1995: 413-22.
18. Alexandra E. Butler, Thomas V. Colby, Laurence Weiss, *et al.* Lymphoepithelioma-like carcinoma of the lung. *Am J Surg Pathol* 1989; 13: 632-9.
19. Han AJ, Xiong M, Gu YY, *et al.* Lymphoepithelioma-like carcinoma of the lung with a better prognosis. A clinico-pathologic study of 32 cases. *Am J Clin Pathol* 2001: 841-50.

罕見的原發性肺部腫瘤：病例報告

陳弘興* 蔡俊明**, ** 彭瑞鵬**, ** 錢尚道*** 許正義****

一個 51 歲已婚男性，因身體健康檢查偶然發現右下肺葉腫瘤。病人不抽煙且除了輕微糖尿病，沒有過去重大病史。沒有呼吸道或全身性症狀。胸部 X 光及電腦斷層等檢查顯示右下肺葉腫瘤，除了疑似右肺門淋巴結腫大，未發現有遠處轉移現象。經手術切除，病理檢查結果為罕見的原發性類淋巴上皮癌 (lymphoepithelioma-like carcinoma of the lung)。原位雜交法 (in situ hybridization) 證實 Epstein-Barr virus 的存在。

原發性類淋巴上皮癌是一種相當罕見的肺部腫瘤。世界衛生組織在 1982 年公佈的肺癌分類上，仍未將此腫瘤列入。在此我們報告這一例罕見的原發性肺癌並探討文獻關於此疾病之特色。(胸腔醫學 2008; 23: 14-18)

關鍵詞：類淋巴上皮癌，EB 病毒，原發性肺癌

* 台北榮民總醫院 胸腔部，** 國立陽明大學醫學院 內科系，*** 國軍高雄總醫院 病理部，

**** 國軍高雄總醫院 胸腔外科

索取抽印本請聯絡：蔡俊明醫師，台北榮民總醫院 胸腔部，台北市石牌路二段 201 號

Obstructive Sleep Apnea in an Obese Patient with Diabetes Mellitus: A Case Report

Li-Chun Huang, Jiunn-Song Jiang, Diana Yuwung Yeh, Shang Jyh Kao, Chia-Mo Lin

Sleep apnea may accelerate metabolic abnormalities, possibly through progressive elevation of stress hormones and cytokines such as cortisol, IL-6 and $\text{TNF}\alpha$. Furthermore, daytime sleepiness is frequently associated with obesity, diabetes, and insulin resistance, independently of sleep disordered breathing.

We herein report an overweight patient with diabetes mellitus who sought help with weight reduction. He was diagnosed with obstructive sleep apnea (OSA), and an uvulopalatopharyngoplasty (UPPP) and tonsillectomy was performed. He experienced significant weight reduction and normalization of blood sugar after the operation. OSA may have been a possible cause of hyperglycemia and obesity in this patient. (*Thorac Med* 2008; 23: 19-24)

Key words: obstructive sleep apnea, obesity, apnea-hypopnea index, continuous positive airway pressure

Introduction

Sleep apnea syndrome, clinically defined by frequent episodes of apnea and hypopnea and symptoms of functional impairment, can be life-threatening and has been associated with extreme daytime hypersomnolence, automobile accidents, and cardiovascular morbidity and mortality [1]. Two percent of women and 4% of middle-aged men in the general population meet the minimal diagnostic criteria for sleep apnea syndrome, with an apnea-hypopnea index (AHI) of 5 or higher and daytime hypersomnolence [2]. Herein, we present the case of a male patient with obstructive sleep apnea (OSA). His obesity and hyperglycemia dramatically improved after his OSA was

treated with uvulopalatopharyngoplasty (UPPP) and tonsillectomy with lateral pharyngeal wall suturing.

Case Report

A 25-year-old obese man was a caregiver with a 6 to 7-year history of bronchial asthma treated with intermittent bronchodilator and steroid inhaler. He also had new-onset type 2 diabetes mellitus controlled with metformin and glimeperide. His family history was unremarkable. He smoked and drank alcohol on social occasions only. He had tried many methods to reduce weight in the past, but without success. Recently, he noted increasing daytime sleepiness. His family

The Division of Chest Medicine, Department of Internal Medicine, Shin Kong Wu Ho-Su Memorial Hospital
Address reprint requests to: Dr. Chia-Mo Lin, Division of Chest Medicine, Department of Internal Medicine, Shin Kong Wu Ho-Su Memorial Hospital, No. 95, Wen-Chang Rd., Shih-Lin District, Taipei City, Taiwan

described heavy snoring and intermittent apnea. Due to increasingly severe symptoms, he was finally referred to the sleep clinic.

On physical examination, he weighed 135 kg; his height was 166 cm with a body mass index (BMI) of 46.7. His tonsils were found to be enlarged bilaterally, and bilateral coarse breathing sounds as well as stridor were present. Baseline blood pressure was in the range of 130-152 mmHg systolic and 80-94 mmHg diastolic. Fasting blood sugar was up to 387 mg/dl with a hemoglobin A1c of 9.4%. Serum cholesterol, triglyceride, cortisol level and thyroid function tests were all within normal limits.

An overnight polysomnography test showed severe sleep apnea (defined as AHI > 30 episodes/hour) with an AHI of 97.1/h and a minimum oxygen desaturation of 46%. He was advised to use bilevel positive airway pressure, but could not tolerate it. A head and neck surgeon was consulted and UPPP with tonsillectomy was arranged (Figure 1 and 2). Post-UPPP and tonsillectomy, continuous positive airway pressure (CPAP) was used short-term and removed on post-operative day 4 because of patient intolerance. However, hypoxemia did not recur, in spite of discontinuing CPAP. At his first follow-up clinical visit on day 12 after the operation, he had lost approximately 20 kg of body weight, with his serum glucose returning to the normal range. The dose of his oral hypoglycemic medications was reduced accordingly. He was advised to monitor his blood glucose and blood pressure closely. His daytime fatigue improved with intensive physical activity, without associated dyspnea. He was also started on a diet with the intention of further weight loss.

At his second follow-up visit on post-op day 21, he had lost a total of 25 kg. His random blood sugar was found to be 74 mg/dl, so he was suggested to follow diet control only. He reported a



Fig. 1. Bilateral enlarged tonsils pre-op



Fig. 2. After UPPP with tonsillectomy



Fig. 3. Obese patient with BMI of 46.7 before UPPP and tonsillectomy



Fig. 4. Significant weight reduction of 50 kg 7 months after UPPP and tonsillectomy

significant reduction of daytime hypersomnolence and snoring; his family also noted fewer apneic episodes and sleep disturbance at night.

Nearly 2 months after UPPP and tonsillectomy, he had lost 40 kg. Seven months later, the patient had lost approximately 50 kg in weight; his BMI was 31.2 kg/m^2 (Figures 3 and 4), random blood glucose was 80 mg/dl, and the hemoglobin A1c was 5.2%. At his follow-up overnight polysomnography study, his AHI dropped to 17.9/h with a minimum O_2 saturation of 81%, significantly improved from his pre-op results. His condition remained stable up to this writing, with no episodes of asthma exacerbation. Further surgical treatment to correct his deviated nasal

septum and chronic sinusitis is being considered.

Discussion

Sleep apnea is one of the leading causes of excessive daytime sleepiness, and may contribute to the development of several cardio-respiratory and metabolic disturbances [1].

Our patient had bilateral tonsillar enlargement and obesity with difficulty in reducing body weight, and type 2 diabetes mellitus. He also complained of daytime sleepiness. OSA produces sleep fragmentation which plays a major role in excessive daytime sleepiness [3]. Progressive deterioration of sleep apnea may accelerate the

worsening of visceral obesity and metabolic syndrome by providing a stress stimulus and causing nocturnal elevations of hormones such as cortisol and insulin [4]. Subjects with OSA are predisposed to weight gain because of daytime somnolence and the decrease in physical activity. Furthermore, sleep apnea is accompanied by potentiated leptin resistance, so that the weight-reducing effects of leptin are especially blunted in OSA [5].

After his work-up, the polysomnography test revealed severe sleep apnea and hypoxia at night. We suggested nasal CPAP treatment initially, which is the mainstay of treatment for OSA [6]; however our patient was unable to tolerate it. Therefore, UPPP and tonsillectomy were performed [7].

When the hypoxemia-reoxygenation stress was taken away by means of UPPP and tonsillectomy, a sustained decrease in body weight to a total of 50 kg was seen within 7 months, and blood glucose normalized off medication. Therefore, correction of OSA resulted in significant weight loss and improvement of diabetes mellitus in this patient. Obesity is the main risk factor for diabetes mellitus, and coexistent severe OSA may add to the risk independently [8].

The main reason for our patient's rapid weight loss 12 days after the operation was most likely increased physical activity and diet control, without his experiencing dyspnea, which were made possible after treating his sleep apnea and sleep fragmentation. In addition, the decreased sympathetic drive resulting in reduced sodium retention and volume expansion could also explain, in part, his rapid weight loss [9]. The patient no longer required the use of bronchodilators and steroid inhalers after UPPP and tonsillectomy, which may imply that some OSA patients in the community may be misdiagnosed with bronchial

asthma when they in fact have OSA.

In conclusion, despite being a common disease, OSA hypopnea syndrome is probably often unrecognized by most primary care physicians. Therefore, an understanding of the complex interaction among sleep, hypersomnolence, sleep-disordered breathing, inflammation, insulin resistance and obesity is necessary to increase awareness of OSA. This may in turn reduce the incidence or severity of OSA-related disorders such as hypertension and diabetes mellitus, which will help in lowering the number of associated adverse cardiovascular complications and automobile accidents.

References

1. Partinen M, Guilleminault C. Daytime sleepiness and vascular morbidity at seven-year follow-up in obstructive sleep apnea patients. *Chest* 1990; 97: 27-32.
2. Bixler EO, Vgontzas AN, Ten Have T, *et al.* Effects of age on sleep apnea in men: Prevalence and severity. *Am J Respir Crit Care Med* 1998; 157: 144-8.
3. Chugh DK, Dinges DF. Mechanisms of sleepiness in obstructive sleep apnea. In: Pack AI ed. *Sleep apnea: pathogenesis, diagnosis and treatment, lung biology in health and disease*. New York; Marcel Dekker, 2002; 265-85.
4. Vgontzas AN, Bixler EO, Chrousos GP. Metabolic disturbances in obesity versus sleep apnea: the importance of visceral obesity and insulin resistance. *J Intern Med* 2003; 254(1): 32-44.
5. O'Donnell CP, Tankersley CG, Polotsky VP, *et al.* Leptin, obesity, and respiratory function. *Respir Physiol* 2000; 119: 163-70.
6. Babu AR, Herdegen J, Fogelfeld L, *et al.* Type 2 diabetes, glycemic control, and continuous positive airway pressure in obstructive sleep apnea. *Arch Intern Med* 2005; 165: 447-52.
7. Kasey K Li. Surgical therapy for obstructive sleep apnea syndrome. *Semin Respir Crit Care Med* 2005; 26(1): 80-8.
8. Elmasry A, Lindberg E, Berne C, *et al.* Sleep-disordered breathing and glucose metabolism in hypertensive men: a

- population-based study. J Intern Med 2001; 249: 153-61.
9. Phillips BG, Kato M, Narkiewicz K, *et al.* Increases in leptin levels, sympathetic drive, and weight gain in obstructive sleep apnea. Am J Physiol 2000; 279: 234-7.

罹患阻塞性睡眠呼吸中止症的肥胖糖尿病病患： 一病例報告

黃麗春 江俊松 葉育雯 高尚志 林嘉謨

睡眠呼吸中止症可加速代謝性異常的原因有可能是因為壓力性荷爾蒙與細胞激素如腎上腺皮質醇，介白素 6 (IL-6) 和腫瘤壞死因子 α (TNF α) 的持續上升所造成。再者，白天昏睡除了睡眠異常呼吸之外，常與肥胖、糖尿病與胰島素抗性相關。我們在此報告一位罹患阻塞性睡眠呼吸中止症的肥胖糖尿病病患到院求助減重的個案。他被診斷為罹患阻塞性睡眠呼吸中止症 (OSA)，併經懸壅垂顎咽整形術與扁桃腺切除術。經開刀後，他減重成功，而且血糖也控制的很好。因此 OSA 有可能是造成這名病患血糖過高與肥胖的原因。(胸腔醫學 2008; 23: 19-24)

關鍵詞：阻塞性睡眠呼吸中止症，肥胖，呼吸中止與淺呼吸指數，連續性呼吸道正壓呼吸

Calcified Pleural Tumor as a Rare Presentation of Paragonimiasis: A Case Report

Chi-Hsien Chen, Jih-Shuin Jerng, Pei-Shin Huang*, Pan-Chyr Yang

Calcified pleural tumor is a rare presentation in paragonimiasis, a parasitic disease that is endemic in Taiwan. The lung and pleura are the most common destinations for the parasite. Pleuropulmonary manifestations have been widely reported, and may mimic several lung diseases, such as lung cancer and pulmonary tuberculosis. The diagnostic requirement is a search for ova in the pleural effusion or pleural tissue. We report a 62-year-old woman who had suffered from intermittent right upper quadrant pain for 7 years. Computed tomography of the chest showed an 8-cm centrally calcified mass lesion in the right costophrenic angle. Biopsy of the mass revealed *Paragonimus westermani* ova surrounded by dense hyalinized fibrotic tissue. This case demonstrates that paragonimiasis may present as a calcified pleural tumor. (*Thorac Med* 2008; 23: 25-30)

Key words: paragonimiasis, *Paragonimus*, pleural, calcification, tumor, abdominal pain

Introduction

Paragonimiasis, a parasitic disease that often causes pleuropulmonary problems, is endemic in the Asia-Pacific area [1]. Although paragonimiasis can be found worldwide, special methods of food preparation in the Asia-Pacific region promote human transmission. In the life cycle of *Paragonimus*, the ingested metacercariae excyst in the gastrointestinal tract, developing into larvae that penetrate the gut, peritoneum, diaphragm, and pleura into the lung. A pleuropulmonary lesion is the most common manifestation of *Paragonimus* infection [1]; its presentation may mimic diseases such as tuberculosis, fungal infection, and malignancy [1-3]. Calcified pleural tumor,

however, is a rare presentation of paragonimiasis. Herein, we describe a patient with pleural paragonimiasis presenting as a calcified pleural tumor initially diagnosed as a chronic post-traumatic intra-pleural hematoma.

Case Report

A 62-year-old woman visited the hospital because of an intermittent dull pain in the right upper costal region after a traffic accident 7 years earlier. The patient recalled a severe bump on her right chest cage shortly after the accident. Chest radiography a month after the accident revealed an 8-cm mass-like lesion with extensive calcification in the right pleural cavity (Figure

Department of Internal Medicine, National Taiwan University Hospital, Taipei, Taiwan, *Department of Pathology, National Taiwan University Hospital, Taipei, Taiwan

Address reprint requests to: Dr. Jih-Shuin Jerng, Department of Internal Medicine, National Taiwan University Hospital, No. 7 Chung-Shan South Road, Taipei 100, Taiwan

1). Post-traumatic intrapleural hematoma was suspected. The pain could be relieved by analgesics, but would recur. Tc-99m DISIDA imaging showed dyskinesia of the gall bladder. Progressive enlargement of the lesion in the non-calcified part was noticed on the annual follow-up radiographs. There was no fever, chills, night sweats or weight loss.

On admission, her temperature was 36.5°C, pulse rate was 72 beats per minute, and respiratory rate was 17 breaths per minute. The patient's blood pressure was 122/72 mmHg and the oxygen saturation was 98% while breathing ambient air. On physical examination, scoliosis was noted, the breathing sound was clear, and there was no chest wall deformity, no lymphadenopathy, and no abdominal tenderness. The hemogram revealed a red blood cell count of 4.41 M/ μ L, hemoglobin of 13.6 g/dl, platelet count of 193 K/ μ L and white blood cell count of 5.49 K/ μ L, with 57.3% poly-

morphonuclear leukocytes, 2.6% eosinophils, and 33.4% lymphocytes. The results of her blood biochemistry were as follows: albumin, 4.4 g/dl; total protein, 7.1 g/dl; blood urea nitrogen, 12.6 mg/dl; serum creatinine, 0.8 mg/dl; sodium, 141 mmol/L; potassium, 3.6 mmol/L; calcium, 2.2 mmol/L; aspartate aminotransferase (AST), 20 U/L; alanine aminotransferase (ALT), 13 U/L; total bilirubin, 0.88 mg/dl; alkaline phosphate (ALP), 112 U/L; gama glutamyl transpeptidase (GGT), 22 U/L; lactate dehydrogenase, 502 U/L, and C-reactive protein, 0.09 mg/dl. Computed tomography showed an 8-cm, contrast-enhanced pleural mass located above the right costophrenic angle, with central calcification and thickened adjacent pleura (Figure 2A, 2B), and an equivocal connection with the twelfth rib (Figure 2C); there was a tiny nodule in the right middle lung (Figure 2D). CT guided biopsy of the mass revealed dense hyaline fibrotic tissues with opercular *P. westermani* ova within the necrotic debris (Figure 3), compatible with paragonimiasis. Surgical intervention was not recommended, and the patient was treated with praziquantel 600 mg daily for 3 days. In the 5-month follow-up, the costal pain had subsided completely, despite the mass size remaining unchanged. The patient was then followed up regularly.

Tracing back her history, she was brought up in Hsinchu County. Freshwater mitten crab has been a popular dish in her family and in that area. She denied having eaten raw crabs in her childhood, but incompletely-cooked crabs or contamination during the cooking process should be considered as possible causes of her parasitic lung disease. She also recalled that her cousin, who lived with her family at that time, had been found to have lung paragonimiasis when she was 7 years old. Her family has not cooked freshwater mitten crabs since then.



Fig. 1. Chest radiography showing an 8-cm mass-like lesion with extensive calcification in the right basal pleural cavity

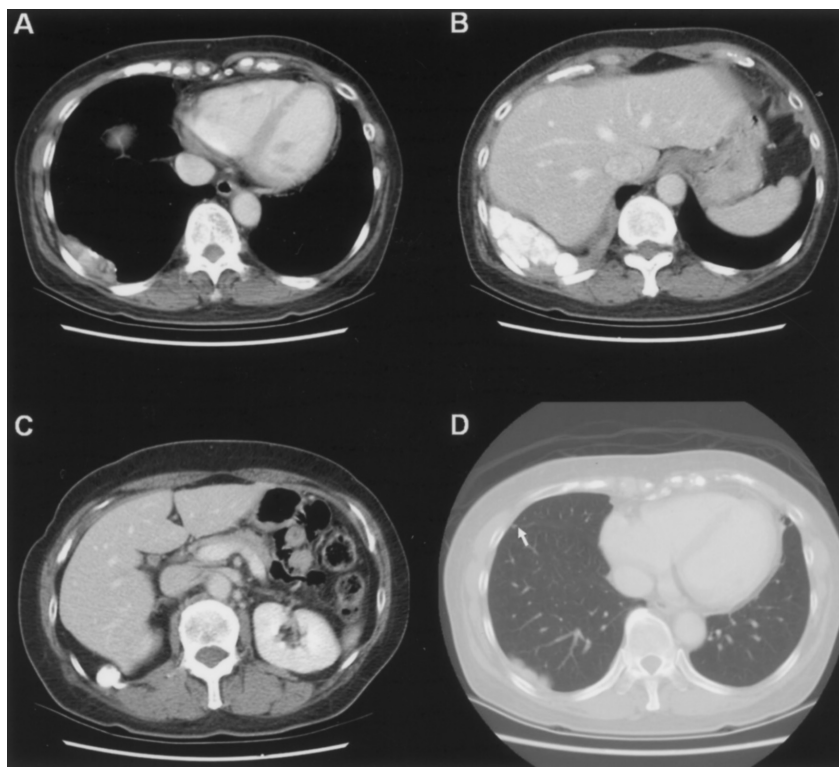


Fig. 2. Chest computed tomography in the mediastinal window. (A) An 8-cm, contrast-enhanced pleural mass located above the right costophrenic angle, with (B) central calcification and thickened adjacent pleura, and (C) an equivocal connection to the 12th rib. (D) In the lung window, a tiny nodule in the right middle lung can be seen (arrow).

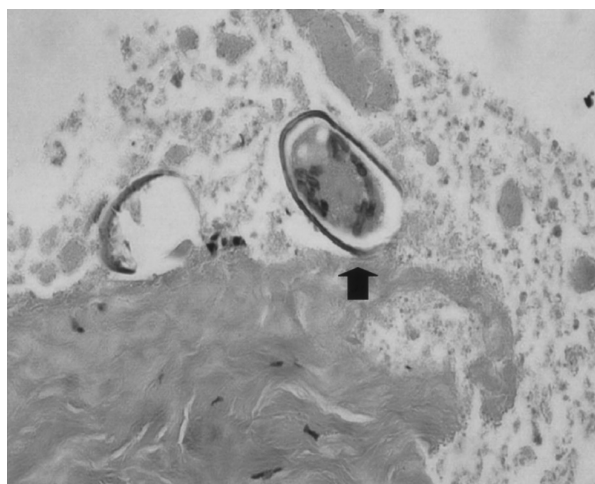


Fig. 3. CT guided biopsy specimen showing dense hyalinized fibrotic tissue admixed with *P. westermani* ova (arrow). Hematoxylin and eosin stain, original magnification, 200 \times .

Discussion

Humans are one of the definitive hosts of *P. westermani*. Ingestion of metacercaria, the infectious form of *Paragonimus* fostered in freshwater crab or crayfish, may lead to permanent mammalian infection. Yokogawa *et al.* has reported that raw crab juice left on the knife or chopping block might contaminate other foods, which then become another infectious route for lung fluke [1]. The larvae might migrate across the diaphragm into the pleural space and enter the lung, where they develop into adult flukes. [1, 4] The mass lesion found at the costophrenic angle in this reported case is explained by their usual migrating route.

The exact life span of *P. westermani* in human beings is not completely understood, but the average life span is usually less than 10 years. There have been reports showing that eggs of *Paragonimus westermani* could be found in sputum 30 years after leaving the endemic area [1]. To our knowledge, this case had the longest latent period (probably more than 50 years) that has been reported in the literature. The calcification may be evidence of a long-term process. However, reinfection cannot be completely ruled out in an endemic area.

The clinical presentation of paragonimiasis depends on the load of larvae and the stage of their migration. Most patients at the early stage experience pleuritic chest pain due to pleurisy. Pleural effusion, hydropneumothorax, or pleural thickening may be found in pleural paragonimiasis [1, 3-7]. After the flukes enter the lung, cough and hemoptysis become the major symptoms [1, 7]. Pulmonary paragonimiasis usually present with a nodule, cyst or mass-like lesion located in the peripheral lung in radiographic studies. In this patient, the nodule in the right middle lung might be considered a pulmonary involvement of paragonimiasis. Although the above presentations may be nonspecific [2, 6], some signs on images may point to the diagnosis of paragonimiasis. A linear opacity in the lung, which suggests a worm migration tract, or a combination of localized pleural thickening and subpleural linear opacities connecting pleura and a necrotic lung nodule were all typical findings of paragonimiasis in chest computed tomography [3, 8].

The differential diagnoses for a calcified pleural tumor might include mesothelioma [9-11], chondrosarcoma, osteosarcoma, ganglioblastoma [12-13], chronic tuberculous or bacterial empyema with fibrothorax [14-15], chronic hematoma [16], and fibrous pseudotumor

of the pleura [17]. This patient had a history of traumatic injury, and recent hematoma, which could also mimic a centrally calcified pleural tumor with diffuse hyperdensity, had once been considered [16]. The attenuation of hematoma on CT scans is mainly contributed to by hemoglobin, and a linear relationship between attenuation and hematocrit has been established [16, 18]. Usually, a search for ova from pleural effusion or biopsy tissue is needed to confirm the diagnosis of paragonimiasis.

Paragonimus may also invade other organs such as the brain, liver, kidney, peritoneum and spinal cord [1], and calcification in the lung, brain, skeletal muscle, and liver has been reported [7, 15]. To our knowledge, paragonimiasis presenting with a calcified pleural mass has never been reported.

Treatment for paragonimiasis with praziquantel has been effective [19-20], but in some patients, bronchiectasis or atelectasis do not recover [7]. The only indication for surgical intervention in this disease is decortication for chronic empyema [7, 21], which was not present in this reported case.

In summary, this case of paragonimiasis with a rare presentation of an extensively calcified pleural mass may alert clinicians to the importance of taking *P. westermani* infection into consideration in patients with chronic calcified pleural lesions.

References

1. Yokogawa M. *Paragonimus* and paragonimiasis. *Adv Parasitol* 1965; 3: 99-158.
2. Minh VD, Engle P, Greenwood JR, *et al.* Pleural paragonimiasis in a Southeast Asia refugee. *Am Rev Respir Dis* 1981; 124(2): 186-8.
3. Kim TS, Han J, Shim SS, *et al.* Pleuropulmonary paragonimiasis: CT findings in 31 patients. *AJR Am J Roentgenol*

- 2005; 185(3): 616-21.
4. DeFrain M, Hooker R. North American paragonimiasis: case report of a severe clinical infection. *Chest* 2002; 121(4): 1368-72.
 5. Ogakwu M, Nwokolo C. Radiological findings in pulmonary paragonimiasis as seen in Nigeria: a review based on one hundred cases. *Br J Radiol* 1973; 46(549): 699-705.
 6. Im JG, Kong Y, Shin YM, *et al.* Pulmonary paragonimiasis: clinical and experimental studies. *Radiographics* 1993; 13(3): 575-86.
 7. Mukae H, Taniguchi H, Matsumoto N, *et al.* Clinicoradiologic features of pleuropulmonary *Paragonimus westermani* on Kyusyu Island, Japan. *Chest* 2001; 120(2): 514-20.
 8. Im JG, Whang HY, Kim WS, *et al.* Pleuropulmonary paragonimiasis: radiologic findings in 71 patients. *AJR Am J Roentgenol* 1992; 159(1): 39-43.
 9. Ng CS, Munden RF, Libshitz HI. Malignant pleural mesothelioma: the spectrum of manifestations on CT in 70 cases. *Clin Radiol* 1999; 54(7): 415-21.
 10. Friedman AC, Fiel SB, Fisher MS, *et al.* Asbestos-related pleural disease and asbestosis: a comparison of CT and chest radiography. *AJR Am J Roentgenol* 1988; 150(2): 269-75.
 11. Quoix E, Chenard MP, Orion B, *et al.* A left pleural effusion with a calcified tumoral mass and left hemithoracic uptake on bone scan. *Lung Cancer* 2001; 32(2): 203-5.
 12. Tateishi U, Gladish GW, Kusumoto M, *et al.* Chest wall tumors: radiologic findings and pathologic correlation: part 2. Malignant tumors. *Radiographics* 2003; 23(6): 1491-508.
 13. Gladish GW, Sabloff BM, Munden RF, *et al.* Primary thoracic sarcomas. *Radiographics* 2002; 22(3): 621-37.
 14. Kim HY, Song KS, Goo JM, *et al.* Thoracic sequelae and complications of tuberculosis. *Radiographics* 2001; 21(4): 839-58; discussion 859-60.
 15. Brown K, Mund DF, Aberle DR, *et al.* radiographic features and differential diagnoses. *Radiographics* 1994; 14(6): 1247-61.
 16. Wolverson MK, Crepps LF, Sundaram M, *et al.* Hyperdensity of recent hemorrhage at body computed tomography: incidence and morphologic variation. *Radiology* 1983; 148(3): 779-84.
 17. Jang KS, Oh YH, Han HX, *et al.* Calcifying fibrous pseudotumor of the pleura. *Ann Thorac Surg* 2004; 78(6): e87-8.
 18. New PF, Aronow S. Attenuation measurements of whole blood and blood fractions in computed tomography. *Radiology* 1976; 121(3 Pt. 1): 635-40.
 19. Johnson RJ, Jong EC, Dunning SB, *et al.* Paragonimiasis: diagnosis and the use of praziquantel in treatment. *Rev Infect Dis* 1985; 7(2): 200-6.
 20. Monson MH, Koenig JW, Sachs R. Successful treatment with praziquantel of six patients infected with the African lung fluke, *Paragonimus uterobilateralis*. *Am J Trop Med Hyg* 1983; 32(2): 371-5.
 21. Dietrick RB, Sade RM, Pak JS. Results of decortication in chronic empyema with special reference of paragonimiasis. *J Thorac Cardiovasc Surg* 1981; 82(1): 58-62.

以鈣化性肋膜腔腫瘤為表現的肺吸蟲症：一病例報告

陳啟信 鄭之勛 黃佩欣* 楊泮池

臺灣地處於肺吸蟲症流行病區，和食用未經熟煮的淡水蝦蟹有關。人類是肺吸蟲的宿主之一，食入的幼蟲會穿過腸道，腹膜，橫隔膜，和肋膜而進入肺臟。因此肺臟和肋膜腔內的變化是肺吸蟲最常見的臨床表現。過去的研究報告顯示，肺吸蟲在肺臟和肋膜腔的表現可以和肺結核與惡性腫瘤相似。而診斷的確立須要經由蟲卵的發現。然而就我們所知，以鈣化的肋膜腔內腫瘤來表現的肺吸蟲症並未被報導過。本個案指出，肺吸蟲症有可以靠近橫隔膜的鈣化腫瘤來表現，且合併長期的右上腹疼痛。(胸腔醫學 2008; 23: 25-30)

關鍵詞：肺吸蟲病，肺吸蟲，胸膜的，鈣化，腫瘤，腹痛

Intramuscular Lipoma Arising in the Intercostal Muscle — A Case Report

Wei-Cheng Lin*, Yih-Leong Chang**, Yung-Chie Lee*,***

Although subcutaneous lipoma is the most common soft tissue neoplasm, deeply-seated intramuscular lipoma is rarely encountered, especially those arising in the chest wall. Because images provide insufficient efficacy to differentiate these benign neoplasms from well-differentiated liposarcomas, excisional biopsy is often needed. Surgical results are markedly good and the recurrence rates depend on free resection margins. We present a rare case of intramuscular lipoma arising in the intercostal muscles. This tumor was found incidentally on the chest roentgenography as a large subpleural mass, and the computerized tomography revealed a well-defined tumor with fatty density straddling the intercostal space. Wide excision of this tumor was performed smoothly, followed by an uneventful course. No local recurrence was noted for 5 years. We report this case with a review of literature. (*Thorac Med* 2008; 23: 31-35)

Key words: intramuscular lipoma, infiltrating lipoma, chest wall tumor

Introduction

Primary chest wall tumors are relatively uncommon and represent from 5% to 44% of all thoracic neoplasms. Of all primary chest wall tumors, 21% to 67% are benign neoplasms. The most common site of involvement is the rib cage and the most common tissue of origin is bone or cartilage. Osteochondroma, chondroma, and fibrous dysplasia are the frequently encountered benign lesions [1].

Soft tissue tumors, including fibromas, lipomas, neurogenic tumors, and vascular tumors, account for 34.8% of all benign chest wall neoplasms [2]. Lipomas are the most common benign

soft tissue neoplasms occurring in every bodily system and location, and about 80% of the lipomas encountered are subcutaneous. Deeply-seated lipomas are uncommon and are usually located within the large muscles of the extremities. Intramuscular lipomas located within the chest walls are very rare, especially those originating from the intercostal muscles. We report a case of intramuscular lipoma arising in the right second intercostal muscles, with a review of the literature.

Case Report

A 50-year-old male patient with buccal

*Division of Thoracic Surgery, Department of Surgery, **Department of Pathology, ***Department of Traumatology, National Taiwan University Hospital and Medical College of National Taiwan University

Address reprint requests to: Dr. Yung-Chie Lee, Division of Thoracic Surgery, Departments of Surgery and Traumatology, National Taiwan University Hospital and Medical College of National Taiwan University, No. 7, Chung Shan South Road, 10002, Taipei, Taiwan

squamous cell carcinoma was incidentally found to have a nodular lesion at the right anterolateral chest wall. The tumor was seated deeply at the right axillary area and was palpable without tenderness in the physical examination. CXR revealed a sharp-margined shadow in the right upper lung field (Figure 1), and chest CT further revealed a ball-sized, well-defined tumor, with density similar to subcutaneous fatty tissue, straddling the intercostal space. (Figure 2) The tumor protruded into the right pleural cavity with a smooth pleural surface, and the nearby ribs were intact. Echo-guided biopsy of this tumor was performed, but adequate tissue could not to be obtained. Therefore, excision of the chest wall



Fig. 1. CXR revealing a sharp-margined shadow at the right upper lung field

tumor was performed. A 7 x 5 x 2 cm tumor at the right second intercostal space was excised. Neither pleura nor rib was invaded by this tumor. Histology revealed a soft tissue mass composed of mature adipose tissue with scattered skeletal muscle fibers (Figure 3), which was compatible with an intramuscular lipoma. The post-operative

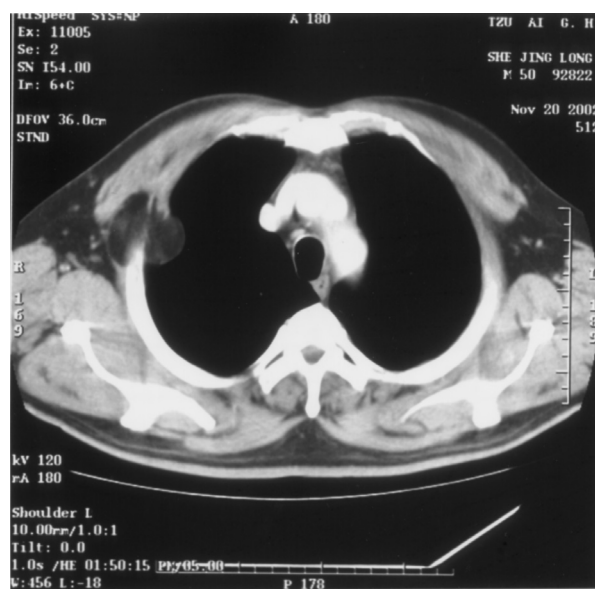


Fig. 2. Chest computed tomography revealing a well-defined tumor straddling the intercostal space. The density of the tumor is similar to subcutaneous fatty tissue and there are focally enhanced materials within the tumor. The tumor protruded into the pleural cavity with a smooth pleural surface.

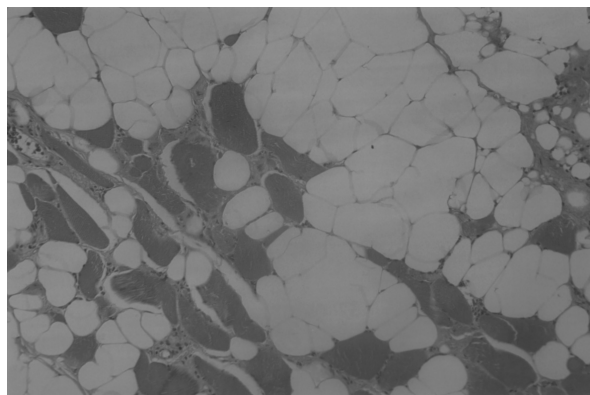


Fig. 3. Microscopically, the tumor is composed of mature adipose tissue with scattered skeletal muscle fibers (H&E, 33x original magnification).

course was uneventful and he was discharged 3 days after operation. No recurrence was noted by the 5-year follow-up.

Discussion

Lipoma is the most common benign soft tissue neoplasm. It can occur in any soft tissue containing fat and affects any age group, with a slight male preponderance. Lipomas usually locate superficially at the subcutaneous layers. A small number of them locate deeply within muscular layers. These deeply-seated lipomas have been well-recognized as a separate entity, known as infiltrating lipomas. They can be intermuscular (arising from the septae between muscles) or intramuscular (arising between muscle fibers). In a review of 2478 adipose tissue tumors, 52 (1.8%) were intramuscular lipomas [3].

Symptoms of intramuscular lipomas depend on the location of the tumors and are secondary to local pressure effects. However, despite arising within the muscles, dysfunction of the muscle or pain (lipoma dolorosa) caused by intramuscular lipoma is rarely encountered. These tumors are generally asymptomatic initially, presenting as a slowly enlarging mass, and are most commonly found in the extremities. Those arising within the chest wall, especially in the intercostal muscles, are rarely reported.

On CT and magnetic resonance imaging, lipomas, including the intramuscular type, approximate fatty tissue. In general, they appear as homogeneous, sharply defined fatty masses. Septations, which may be thin fibrous bands or thicker muscle bundles, are not uncommon, but make it impossible to rule out well-differentiated liposarcoma on the basis of imaging alone [4].

Well-differentiated liposarcomas, or atypical lipomatous tumors, have the potential to exhibit

locally aggressive behavior, such as local recurrence, but have no metastatic potential. Bassett *et al.*, observed that 4% of patients with intramuscular lipomas had disease recurrence, whereas 27% of patients with well-differentiated liposarcoma had disease recurrence after marginal resection [5]. There is some overlap of the clinicohistologic and karyotypic features between intramuscular lipomas and well-differentiated liposarcomas. In Bassett's study, 6 of 57 patients (10%) originally classified as having intramuscular lipoma were reclassified as having well-differentiated liposarcoma after detailed observation of their karyotypes [5].

Since there are no reliable clinical features for distinguishing intramuscular lipoma from well-differentiated liposarcoma, complete surgical excision is mandatory for a definite histological diagnosis and curative treatment.

The overall recurrence rate reported in the literature varies from 3.0% to 62.5%, and the most important factor is complete resection. In 1 study, intramuscular lipomas were further divided into 2 subtypes: infiltrative and well-circumscribed, with respective local recurrence rates being 19% and 0% [3]. Similar histologic features and their relation to local recurrence were also observed in another study [5]. The infiltrating growth characteristic of infiltrative intramuscular lipoma may be associated with type-selective muscular degeneration and endomysial fatty growth as a result of focal atrophy [6]. However, the primary cause of focal muscle involution is not well comprehended. Fortunately, despite tissue infiltration, no malignant transformation has been reported.

In conclusion, we reported a rare case of intramuscular lipoma arising at the intercostal muscles, which was completely excised without recurrence for 5 years. Intramuscular lipoma is indistinguishable from well-differentiated

liposarcoma by the clinical presentation and imaging appearance. Complete excision offers a definite diagnosis and curative treatment.

References

1. Bernard J Park VWR. Chest Wall Tumors. In: Thomas WS JL, Ronald BP, Valerie WR ed. General Thoracic Surgery. Lippincott Williams & Wilkins, Philadelphia, 2005; 710-21.
2. Athanassiadi K, Kalavrouziotis G, Rondogianni D, *et al.* Primary chest wall tumors: early and long-term results of surgical treatment. *Eur J Cardiothorac Surg* 2001; 19: 589-93.
3. Fletcher CD, Martin-Bates E, Fletcher CD, *et al.* Intramuscular and intermuscular lipoma: neglected diagnoses. *Histopathology* 1988; 12: 275-87.
4. Keogh C, Torreggiani WC, Al-Ismail K, *et al.* Musculoskeletal case 24. Intramuscular lipoma. *Can J Surg* 2002; 45: 367.
5. Bassett MD, Schuetze SM, Distèche C, *et al.* Deep-seated, well differentiated lipomatous tumors of the chest wall and extremities: the role of cytogenetics in classification and prognostication. *Cancer* 2005; 103: 409-16.
6. Mori K, Chano T, Matsumoto K, *et al.* Type-selective muscular degeneration promotes infiltrative growth of intramuscular lipoma. *BMC Musculoskelet Disord* 2004; 5: 20.

肋間肌肉肌內脂肪瘤—病例報告

林洧呈* 張逸良** 李元麒*,***

肌內脂肪瘤是一種罕見而有其特殊臨床及病理表現的脂肪瘤類型，而發生於肋間肌肉者則未見於現有文獻之中。由於在臨床症狀和影像檢查上，我們難以區分良性肌內脂肪瘤和惡性的高度分化肌肉瘤，所以廣泛手術切除是最好的診斷與治療方式。在此一病例報告中，我們呈現一個50歲男性病患在例行胸部X光檢查中，意外發現一個右上肺野腫瘤。胸部電腦斷層顯現一個橫跨肋間的軟組織腫瘤伴隨完整的肋膜表面。病患隨後接受此胸壁腫瘤的廣泛切除。病理檢查報告為一肌內脂肪瘤。病患術後恢復良好，在5年的術後追蹤期間並無復發。除了報告此一罕見病例，我們也回顧整理現有的相關文獻。(胸腔醫學 2008; 23: 31-35)

關鍵詞：肌內脂肪瘤，胸壁腫瘤

* 國立台灣大學醫學院附設醫院 外科部胸腔外科，** 國立台灣大學醫學院附設醫院 病理部，

*** 國立台灣大學醫學院附設醫院 創傷醫學部

索取抽印本請聯絡：李元麒醫師，國立台灣大學醫學院附設醫院 外科部胸腔外科，台北市中山南路7號

Primary Small Cell Carcinoma of the Esophagus: Two Case Reports

Chia-Hung Sun*, Shinn-Liang Lai**,***, Reury-Perng Perng**,***

Primary small cell carcinoma (SCC) is a rare entity in the esophagus, although it is relatively common in the lung. Similar to small cell lung carcinoma, SCC of the esophagus is aggressive and the prognosis is poor. In this article, we report 2 patients with primary SCC of the esophagus with distal metastasis. They received chemotherapy and radiotherapy, and survived for 6 months and 10 months, respectively. (*Thorac Med* 2008; 23: 36-41)

Key words: small cell carcinoma, esophagus, chemotherapy, radiotherapy, surgery

Introduction

Primary small cell carcinoma (SCC) of the esophagus is a rare and aggressive tumor with early distant metastasis [1]. Its natural history is somewhat similar to that of small cell lung carcinoma [2-4]. The standard of treatment has not yet been established due to the paucity of cases. Its prognosis is poor because of its aggressive nature and the high incidence of distant metastasis to the liver, lung, bone, and brain [5]. In this report, we present our experience with 2 patients diagnosed with SCC of the esophagus in our hospital. One patient who was diagnosed with SCC of the esophagus with mediastinal lymphadenopathy, lung and brain metastasis and who received chemotherapy and radiotherapy had a survival of 10 months. The other patient was diagnosed with SCC of the esophagus with retroperitoneal carcinomatosis, and liver and bone metas-

tasis, and survived 6 months.

Case Reports

Case 1

A 73-year-old man was a current smoker. He was referred to our hospital in Dec. 2005 due to dysphagia for 3 months. Upper gastrointestinal (GI) endoscopy showed an esophageal tumor and gastroesophageal reflux disease. Biopsy from the tumor demonstrated small cell carcinoma. The chest X-ray (CXR) showed increased soft tissue density in the right upper mediastinum (Figure 1A). The chest computed tomography (CT) scan revealed a 4.0 cm segmental wall thickening of the upper and middle thirds of the esophagus, and multiple mediastinal lymph nodes enlargement, with the largest one, about 5.0 x 4.0 x 5.4 cm, in the right upper paratracheal region (Figure 1B). With the diagnosis of extensive-stage

*Department of Internal Medicine, Taipei City Hospital, Taiwan, **Chest Department, Taipei Veterans General Hospital, Taiwan, ***School of Medicine, National Yang-Ming University, Taipei, Taiwan
Address reprint requests to: Dr. Shinn-Liang Lai, Chest Department, Taipei Veterans General Hospital, 201, Section 2, Shih-Pai Road, Taipei 112, Taiwan



Fig. 1A. Chest X-ray showing an increased soft tissue density in the right upper mediastinum (arrow).



Fig. 1B. Chest computed tomography scan revealed a mass lesion about 4.0 cm in diameter in the upper esophagus (arrow), and multiple enlarged mediastinal lymph nodes in the right upper paratracheal region.

esophageal primary SCC with mediastinal lymphadenopathy and lung metastasis, the patient received chemotherapy with a cisplatin (60 mg/M², day 1) and etoposide (60 mg/M², day 1-3) combination for 2 cycles. Because of disease progression with tumor enlargement, the regimens of chemotherapy were changed to a combination of ifosfamide (1000 mg/M², day 1-3) and oral etoposide (50 mg qd, day 4-13) for 2 cycles. Follow-up CXR showed stable tumor disease.

The chemotherapy regimen was switched to a paclitaxel (150 mg/M², day 1) and carboplatin (175 mg/M², day 2) combination for 2 cycles. However, tumor progression with supraclavicular lymphadenopathy developed in Aug. 2006. Palliative radiotherapy was arranged to cover the bilateral supraclavicular region and mid-third of the esophagus (3000 cGy). In Sep. 2006, the patient complained of headache and unsteady gait. Brain CT and magnetic resonance imaging (MRI) demonstrated multiple nodular lesions in the bilateral cerebral hemispheres, cerebellar hemispheres, and brain stem which were compatible with brain metastasis of SCC. Whole brain irradiation up to 3000 cGy was scheduled for palliative purposes. Chemotherapy was adjusted to combined epirubicin (20 mg/M², day 1) and topotecan (1.5 mg/M², days 1-3) for 1 cycle. Unfortunately, the patient's condition worsened gradually in Oct. 2006 with the presentations of poor appetite, dyspnea, drowsy consciousness, pancytopenia, and renal function impairment. He expired on 10 Oct. 2006, after 10 months of survival.

Case 2

A 52-year-old man with a past history of alcohol-related chronic pancreatitis was a current smoker. He was admitted to our hospital in May 2006 due to abdominal pain, poor food intake, nausea after meals, and body weight loss of about 5 kilograms in the most recent 2 weeks. Serum amylase was 220 U/L, lipase 205 U/L, aspartate aminotransferase 66 U/L, alanine aminotransferase 30 U/L, alkaline phosphatase 364 U/L, and γ -glutamyl transpeptidase was 548 U/L. Abdominal CT scan revealed a mass lesion about 7.0 cm in diameter in the esophagus with ulceration from the subcarinal level caudally to the cardiac portion, extensive lymphadenopathy in the

mediastinum, lower neck, abdominal cavity, and retroperitoneum, peritoneal tumor carcinomatosis and ascites, multiple small poorly enhanced nodules in the liver, and osteolytic lesions in the thoracic vertebral bodies (Figure 2A). Upper gastrointestinal endoscopy showed a huge ulcerated mass at the lower third of the esophagus. Biopsy of the esophageal tumor demonstrated SCC which presented scanty cytoplasm, a highly hyperchromatic oval-to-elongated nucleus, and positive immunostaining for cytokeratin and chromogranin (Figure 2B). The whole body bone scan revealed multiple foci of increased radioactivity involving the skull, spine, right clavicle, and rib cages. Therefore, the patient was diagnosed to have primary SCC of the esophagus with liver and bone metastasis, peritoneal carcinomatosis, and mediastinal and retroperitoneal lymphadenopathy. Initial chemotherapy was started with a cisplatin (60 mg/M², day 1) and etoposide (60 mg/M², day 1-3) combination for 5 cycles. Follow-up chest CT scan in Sep. 2006 disclosed regressive change in the tumor volume of the esophageal cancer, but there were progressive changes in the mediastinal lymphadenopathy, and

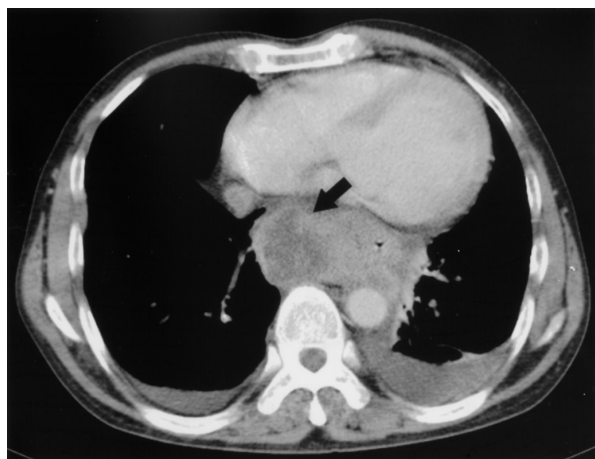


Fig. 2A. Abdominal computed tomography scan revealed an ulcerative mass lesion about 7.0 cm in diameter in the esophagus (arrow) with extensive mediastinal lymphadenopathy.

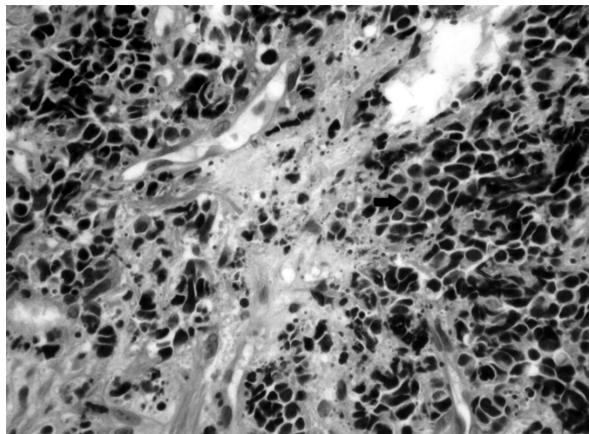


Fig. 2B. Biopsy of the esophageal tumor demonstrated small cell carcinoma (arrow) which presented scanty cytoplasm, and a highly hyperchromatic oval to elongated nucleus (H&E stain, 400X).

liver and right adrenal metastasis. Chemotherapy regimens were switched to combined ifosfamide (1000 mg/M², days 1-3) and oral etoposide (50 mg qd, days 4-13) for 1 cycle. Unfortunately, the patient suffered from progressive general weakness and poor appetite in Nov. 2006. He was admitted due to pneumonia with septic shock and acute respiratory failure. After cardiopulmonary resuscitation, the man expired on 29 Nov. 2006. The survival time was 6 months.

Discussion

Primary SCC of the esophagus is a rare histological type of esophageal carcinoma. Since McKeown first described 2 autopsy cases of esophageal SCC, only approximately 230 cases have been reported as of 1995 [6]. The incidence of esophageal tumor has been estimated to range from 0.8% to 2.4% of all esophageal malignancies [7-8]. The current results reveal that the natural history of primary SCC of the esophagus is somewhat comparable to the natural history of SCC of the lung, and that the extent of disease is an important factor for predicting survival [9].

In a review of patients with esophageal SCC, the reported risk factors included smoking, alcohol, ulcerative colitis, choledochal cyst, immunosuppression, and male gender [1, 10-11]. Our 2 patients were both male current smokers and 1 of them was an alcoholic. They seemed to have the reported risk factors.

Esophageal SCC is preferentially located in the middle and lower esophageal segment [4, 12]. The initial symptoms of esophageal SCC do not differ from those of more frequent histological types. The most common symptoms are dysphagia and body weight loss [7]. Its clinical presentations are almost always more aggressive and are related to the extent of the disease. The initial symptom of our 2 patients was dysphagia, which was compatible with reported experience.

An upper GI endoscopy is usually required for identification and biopsy of the primary tumor. Image surveys and other studies are helpful in defining the extent of disease. On diagnosis, 50% to 70% of patients are found to have distant metastasis [3, 13-14]. Limited disease is defined as a tumor mass confined within the esophagus or periesophageal tissues, with or without regional lymph node metastasis (T1-4N0-1). Extensive disease is defined as a tumor outside the locoregional area (e.g., liver, bone, or distant lymph node metastasis [any T, any N, M1]) [15-16]. Based on this staging criterion, our 2 cases were extensive disease esophageal SCC.

The optimal treatment for patients with primary SCC of the esophagus has not been established due to the limited available data. Known for its unfavorable prognosis, combined modality therapy for SCC has been used increasingly, with radiation therapy and surgery for local disease control and platinum-based chemotherapy for systemic disease control. In general, patients with limited-stage disease usually receive a combined

modality of management, whereas patients with extensive-stage disease primarily receive chemotherapy [2, 8-9]. The initial regimens of chemotherapy for our 2 patients were a combination of cisplatin and etoposide. However, the responses were poor. Smoking, advanced disease, and old age might have contributed to their unfavorable prognosis.

With the disappointing management results, the outcomes of esophageal SCC are usually poor. This is reflected in a median survival of 6.2 months (range 0-33 months) in a review of 162 reported cases [17]. Casas and colleagues collected data on 199 patients and estimated that the median survival time for patients with limited disease was 8 months, while the patients with extensive disease survived 3 months [3].

In summary, primary small cell carcinoma of the esophagus is a rare and aggressive disease. Metastatic dissemination often preexists at diagnosis, which results in a poor prognosis. To our knowledge, the treatment strategy is often selected according to the condition of the lung, but the outcomes are always unsatisfactory. Further prospective studies will be required to obtain a better understanding of this entity and the optimal therapy.

References

1. Bennouna J, Bardet E, Deguiral P, *et al.* Small Cell Carcinoma of the Esophagus: Analysis of 10 Cases and Review of the Published Data. *Am J Clin Oncol* 2000; 23: 455-9.
2. Law STK, Fok M, Lam KY, *et al.* Small cell carcinoma of the esophagus. *Cancer* 1994; 73: 2894-9.
3. Casas F, Ferrer F, Farrus B, *et al.* Primary small cell carcinoma of the esophagus: a review of the literature with emphasis on therapy and prognosis. *Cancer* 1997; 80: 1366-72.
4. Huncharek M, Muscat J. Small cell carcinoma of the esophagus. The Massachusetts General Hospital experience,

- 1978 to 1993. *Chest* 1995; 107: 179-81.
5. Matsuoka M, Boku N, Yoshino T, *et al.* Small cell carcinoma of the esophagus responding to fourth-line chemotherapy with weekly paclitaxel. *Int J Clin Oncol* 2005; 10: 429-32.
6. McKeown F. Oat cell carcinoma of the esophagus: *J Pathol Bacteriol* 1952; 64: 889-91.
7. Beyer KL, Marshall JB, Diaz-Arias AA, *et al.* Primary small cell carcinoma of the esophagus. *J Clin Gastroenterol* 1991; 13: 135-41.
8. Nishimaki T, Suzuki T, Nakagawa S, *et al.* Tumor spread and outcome of treatment in primary esophageal small cell carcinoma. *J Surg Oncol* 1997; 64: 130-4.
9. Haider K, Shahid RK, Finch D, *et al.* Extrapulmonary Small Cell Cancer: A Canadian Province's Experience. *Cancer* 2006; 107: 2262-9.
10. Brenner B, Laura TH, Klimstra DS, *et al.* Small-cell carcinoma of the gastrointestinal tract: a review. *J Clin Oncol* 2004; 22: 2730-9.
11. Remick SC, Hafez GR, Carbone PP. Extrapulmonary small cell carcinoma. A review of the literature with emphasis on therapy and outcome. *Medicine* 1987; 66: 457-71.
12. Nichols GL, Kelsen DP. Small cell carcinoma of the esophagus: the Memorial Hospital experience 1970 to 1987. *Cancer* 1989; 64: 1531-3.
13. Craig SR, Carey FA, Walker WS, *et al.* Primary small cell carcinoma of the esophagus. *Thorac Cardiovasc Surg* 1995; 109: 284-8.
14. Nemoto K, Zhao HJ, Goto T, *et al.* Radiation Therapy for Limited-Stage Small-Cell Esophageal Cancer. *Am J Clin Oncol* 2002; 25(4): 404-7.
15. Medgyesy CD, Wolff RA, Putnam JB Jr, *et al.* Small Cell Carcinoma of the Esophagus. *Cancer* 2000; 88: 262-7.
16. Fleming ID, Cooper JS, Henson DE, *et al.* Digestive System. Esophagus. In: American Joint Committee on Cancer staging manual. 5th edition. Philadelphia: Lippincott-Raven 1997: 65-8.
17. Paraf F, Serre I, Sarfati E, *et al.* Carcinome neuroendocrine de l'oesophage. *Ann Chir* 1990; 44: 249-51.

原發性食道小細胞癌：二個病例報告

孫嘉宏* 賴信良**,*** 彭瑞鵬**,***

雖然原發性小細胞癌在肺內相當常見，但是在食道內為一少見惡性本質。類似於肺小細胞癌，食道小細胞癌具有侵襲性而且預後差。本篇文章中，我們報告二位原發性食道小細胞癌合併早期遠處轉移的病人，他們接受化學治療及放射治療，存活率分別為六個月及十個月。(胸腔醫學 2008; 23: 36-41)

關鍵詞：小細胞癌，食道，化學治療，放射治療，手術

* 台北市立醫院 內科部，** 台北榮民總醫院 胸腔部，*** 國立陽明大學醫學院

索取抽印本請聯絡：賴信良醫師，台北榮民總醫院 胸腔部，112 台北市北投區石牌路二段 201 號 14 樓

Pulmonary Metastatic Malignant Peripheral Nerve Sheath Tumor in an Adult Patient with Neurofibromatosis Type I — A Case Report

Cheng-Yu Chang, Chen-Tu Wu*, Ching-Hung Lin**, Chao-Chi Ho***,
Pan-Chyr Yang***

Neurofibromatosis type I (NF1) or von Recklinghausen's disease is an autosomal dominant disease with a frequency of 1 in 3000. Malignant peripheral nerve sheath tumors (MPNSTs) are rare spindle cell sarcomas, derived from Schwann cells or pluripotent cells of the neural crest. Some of these tumors occur in association with neurofibromatosis type 1 (NF1). MPNSTs are usually resistant to chemotherapy or radiotherapy, and those associated with NF1 behave in a more aggressive way. We report a rare case of a NF1 patient with respiratory failure caused by metastatic pulmonary MPNST, who was successfully treated by combination chemotherapy. (*Thorac Med* 2008; 23: 42-48)

Key words: neurofibromatosis, NF1, soft tissue sarcoma, neurofibrosarcoma, malignant peripheral nerve sheath tumor

Introduction

Neurofibromatosis type I (NF1) also known as von Recklinghausen's disease, is an autosomal dominant disease with an incidence of 1 in 3000 [1]. Patients with NF1 have an increased risk of malignancy as compared with those in the general population [2]. Malignant peripheral nerve sheath tumors (MPNSTs; formerly called neurofibrosarcoma) are rare neoplasms, at least 4% of patients with NF1 may develop MPNSTs [3]. Survival after the development of pulmonary metas-

tasis is poor [4-5].

The identification of neurogenic malignant tumor is difficult when depending on the histological pattern alone. Immunocytochemical techniques using S-100 antigen are valuable in assisting the diagnosis of peripheral nerve sheath tumors [6-7]. PET imaging and MRI are also helpful in demonstrating malignant transformation [8]. Local excision alone has a high failure rate, but multiplicity treatment shows evidence of decreased recurrence [3]. Radiotherapy was controversially recommended for local recur-

Division of Pulmonary Medicine, Department of Internal Medicine, Far Eastern Memorial Hospital, Taipei, Taiwan, *Department of Pathology, National Taiwan University Hospital and National Taiwan University College of Medicine, Taipei, Taiwan, **Department of Oncology, National Taiwan University Hospital and National Taiwan University College of Medicine, Taipei, Taiwan, ***Department of Internal Medicine, National Taiwan University Hospital and National Taiwan University College of Medicine, Taipei, Taiwan

Address reprint requests to: Dr. Ching-Hung Lin, Department of Oncology, National Taiwan University Hospital and National Taiwan University College of Medicine, No. 7, Chung-Shan South Road, Taipei 100, Taiwan

ence and unresectable lesions [6]. In recent studies, chemotherapy with adriamycin combined with cyclophosphamide or vincristine had a 46% response rate with metastatic MPNSTs [9]. Herein, we report a patient with NF1, who suffered from acute respiratory failure due to pulmonary involvement of MPNST. The patient was successfully weaned from the ventilator after chemotherapy.

Case Report

A 55-year-old female housekeeper had been a patient with neurofibromatosis type I since early childhood, but without a family history. An enlarging hard left leg mass developed in the most recent 1 year, without local tenderness. Two months before admission, she suffered from productive cough and progressive exertional dyspnea. The chest radiography (Figure 1) showed bilateral multiple lung nodules with pleural effusion.

On admission, a huge left leg mass (15 x 10

cm in size, Figure 2) was found just below the knee in addition to café-au-lait spots on the face, trunk and extremities. Neurological examination found the cranial nerves to be intact. Arterial blood gas while receiving oxygen at 3L/min showed pH 7.43; PaO₂ 58.9 mmHg; PaCO₂ 45.3 mmHg; bicarbonate 29.3 mEq/l; and oxygen saturation at 91%.

The chest computed tomography (CT) (Figure 3A) showed multiple nodules with mild enhancement at the bilateral lungs, pleural spaces and skin of the chest wall. Magnetic resonance imaging (MRI) (Figure 4) of the extremities demonstrated left leg multiple plexiform soft tissue tumors, most likely neurogenic tumors. The largest was about 11.4 x 7.3 x 5 cm in size, with

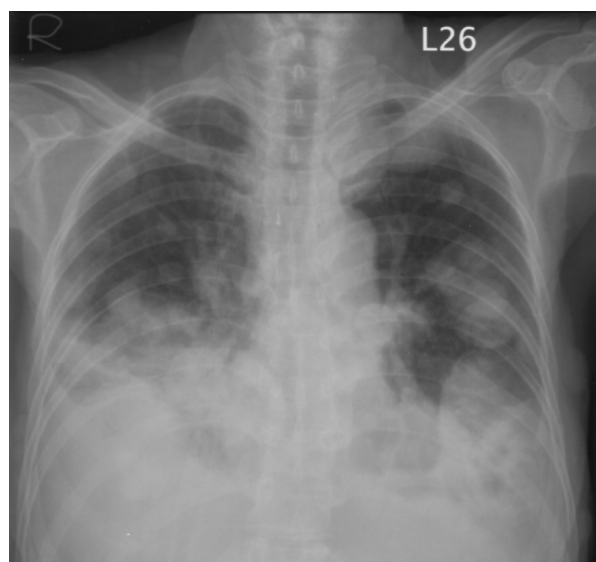


Fig. 1. Chest X-ray shows bilateral multiple lung nodules with pleural effusion.



Fig. 2. Grossly observed, the left leg mass was huge without skin defect.



Fig. 3A. Chest CT with contrast shows multiple nodules with bilateral mild enhancement at the lung, pleural spaces and dermis of the chest wall.



Fig. 3B. Chest CT with contrast shows lung nodules decreasing in size after 4 courses of chemotherapy.

varying degrees of cystic change. Ill-defined enhancements involved the proximal tibia at the epi-metaphysis and middle shaft. Percutaneous needle biopsy of the lung nodules revealed oval to spindle hyperchromatic tumor cells with mito-

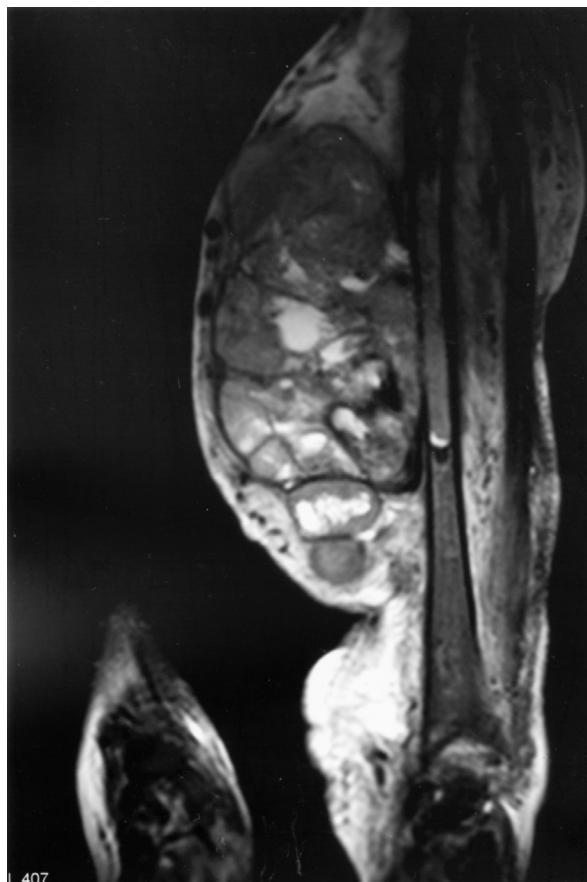


Fig. 4. T-1 weighted magnetic resonance image with contrast shows multiple lobular plexiform soft tissue tumors with tibial destruction.

tic figures. Immunohistochemically, the tumor cells were strongly positive for vimentin and focally positive for CD99 but negative for cytokeratin, S-100 protein and smooth muscle actin. The histopathological features favored a primitive sarcoma (Figure 5). Ten days after admission, the patient had rapid shallow respiration and deterioration of consciousness. Follow-up CXR showed diffuse pulmonary metastasis and massive pleural effusion. The arterial blood gas analysis reported: pH 7.26; PaO₂ 85.3 mmHg; PaCO₂ 95.2 mmHg; sodium bicarbonate 11.3 mEq/l; and oxygen saturation of 95%. She was intubated because of hypercapnic respiratory failure.

Percutaneous fine needle biopsy of the left

leg tumor was used to search for a possible primary lesion causing the metastasis. The histopathological features revealed pleomorphic tumor cells containing irregularly ovoid or spindle nuclei positive for vimentin and CD99 in the tumor cells, which were similar to those in the lung nodules. In addition, S-100 protein reactivity was shown in the left leg tumor (Figure 6). The clinical, radiologic and histopathological features pointed toward an MPNST. The patient received 2 chemotherapy cycles of reduced dose IE (ifosfamide 3000 mg/m², etoposide 80 mg/m²),

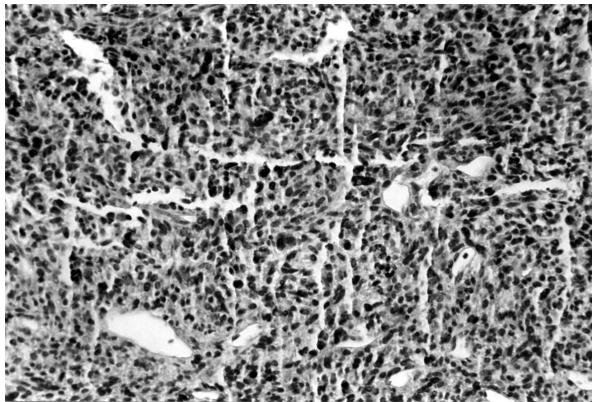


Fig. 5. Oval to spindle hyperchromatic tumor cells in the lung tumor tissue (hematoxylin and eosin, 66x original magnification).

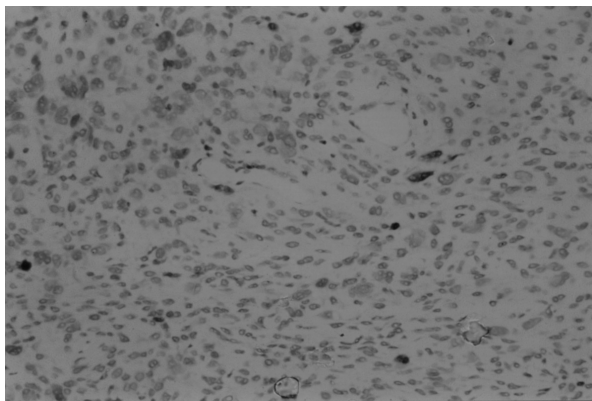


Fig. 6. Pleomorphic sarcomatous cells in the leg lesion demonstrate irregular sizes and shapes of hyperchromatic nuclei, sometimes in a wavy shape. The tumor cells are focally S-100 protein reactive (ABC method, 66x original magnification).

but the tumor size did not change. Therefore, tracheostomy was performed due to prolonged intubation. She received 2 other cycles of salvage chemotherapy with CEV (cyclophosphamide 1000 mg/m², epirubicin 80 mg/m², vincristine sulfate 2 mg), and the tumor size decreased gradually. (Figure 3B) She was weaned off the ventilator smoothly within 1 month.

Discussion

Neurofibromatosis type I (NF1), or von Recklinghausen's disease, is an autosomal dominant disease with a frequency of 1 in 3000. The most common presentations were cutaneous café-au-lait spots and neurofibromas of the peripheral nerves [1, 11-12]. The NF1 gene on chromosome 17q11.2 is a tumor suppressor gene, and mutation of this gene results in malignant transformation [8, 13]. A rapidly growing neurofibroma or local pain may be related to malignant transformation or internal bleeding [3]. In our case, a left leg mass rapidly enlarged within 1 year, which led to further evaluation and the confirmation of an MPNST.

Pulmonary manifestations in NF1 include thoracic neoplasm, interstitial lung disease, kyphoscoliosis and cutaneous neurofibromas. NF1-related interstitial lung disease (ILD) is characterized by upper lobe bullous change and basilar fibrosis [14]. Primary pulmonary sarcoma complicating NF1 is a rare malignancy, and most of the pulmonary tumors are metastatic lesions [15]. After malignant transformation, metastasis to the lung may occur rapidly, as in our present patient [16].

In 1952, Preston *et al.* reported 61 male patients with NF1, and 10 of them developed sarcoma [17]. In 678 NF1 patients reviewed by D'Agostino *et al.*, 12 had neurofibrosarcoma of

the somatic tissues or peripheral nerves [4]. In a 39-year follow-up study, cancer developed in one-third of the NF1 patients, and the total relative risk was 2.5 (confidence interval, 1.9 to 3.3), especially in female patients [2]. Madeleine and Birgitta reported a Swedish population study, in which 24% of NF1 patients developed malignant tumors after 12 years of follow-up. Among these 70 NF1 patients, 5 had soft tissue sarcoma (7%) and only 1 had neurofibrosarcoma with lung metastasis [18].

The neurofibrosarcoma demonstrates soft tissue heterogeneous density on CT with contrast enhancement, and possible bony destruction [19]. Microscopically, neurogenic sarcoma presented oval to spindle hyperchromatic tumor cells with mitotic figures and varying degrees of nuclear pleomorphism [4, 20]. Recently, immunocytochemical techniques using S-100 antigen have supported the diagnosis of MPNSTs, especially in cases only receiving fine needle aspiration cytology. However, S-100 antigen is only reactive in half of MPNSTs [6-7].

The most common cause of death in patients of NF1 is malignancy. The poor prognostic factors of MPNST include: larger tumors, local recurrence, distant metastasis, and a high histopathologic grade. Pulmonary metastasis is an especially poor indicator. Tumor local recurrences have an ominous prognosis in NF1 patients. Approximately 50% of patients with malignant neurofibrosarcoma of NF1 died within 1 year after local recurrence [4-5]. Local excision alone had a high failure rate, and multiplicity of treatment had evidence of decreased local recurrence [6]. In patients with moderate to high grade neurofibrosarcoma, neoadjuvant chemotherapy and radiation therapy followed by wide excision and adjuvant chemotherapy have been reported to achieve local disease control and prolonged sur-

vival [3]. Adriamycin combined with cyclophosphamide or vincristine therapy had a 46% response among 46 patients with metastatic neurofibrosarcoma [9]. Our patient received 2 cycles of chemotherapy with ifosfamide and etoposide, followed by 2 cycles of cyclophosphamide, epirubicin and vincristine sulfate. The follow-up chest CT showed that the lung tumors had decreased in size and she was successfully weaned off the mechanical ventilator.

Conclusion

We presented a rare pulmonary manifestation of NF1 complicated with metastatic peripheral nerve sheath tumor. Combination chemotherapy showed a good response for pulmonary metastasis. Because the development of malignancy is part of the NF1 process, a rapidly growing neurofibroma or pain development should prompt an immediate evaluation.

References

1. Crowe FW, Schull WJ, Neel JV. A clinical pathological genetic study of multiple neurofibromatosis. Springfield, III: Charles C Thomas, 1956; 1-176.
2. Sorensen SA, Mulvihill JJ, Nielsen A. Long-term follow-up of von Recklinghausen's neurofibromatosis. *N Engl J Med* 1986; 314: 1010-5.
3. Storm F, Eilber F, Mira J, *et al.* Neurofibrosarcoma. *Cancer* 1980; 45: 126-29.
4. D'Agostino AN, Soule EH, Miller RH. Sarcomas of the peripheral nerves and somatic soft tissues associated with multiple neurofibromatosis (von Recklinghausen's disease). *Cancer* 1963; 16: 1015-27.
5. Sordillo PP, Helson L, Hajdu SI, *et al.* Malignant Schwannoma—clinical characteristics, survival, and response to therapy. *Cancer* 1981; 47: 2503-9.
6. Bailet JW, Abemayor E, Andrews JC. Malignant nerve sheath tumors of the head and neck: a combined experience from two university hospitals. *Laryngoscope* 1991; 101:

- 1044-9.
7. Diamaru Y, Hashimoto H, Enjoji M. Malignant peripheral nerve-sheath tumors (malignant Schwannomas): An immunohistochemical study of 29 cases. *Am J Surg Pathol* 1985; 9: 434-44.
 8. Yohay K. Neurofibromatosis types 1 and 2. *Neurologist* 2006; 12: 86-93.
 9. Wilbur JR, Sutow WW, Sullivan MP, *et al.* Chemotherapy of sarcomas. *Cancer* 1975; 36: 765-9.
 10. Stout, AP. Peripheral manifestation of the specific nerve sheath tumor (neurilemoma). *Am J Cancer* 1935; 24: 751-96.
 11. Gutmann DH, Aylsworth A, Carey JC, *et al.* The diagnostic evaluation and multidisciplinary management of neurofibromatosis 1 and neurofibromatosis 2. *JAMA* 1997; 278: 51-7.
 12. Riccardi VM. Von Recklinghausen neurofibromatosis. *N Engl J Med* 1981; 305: 1617-27.
 13. Crawford AH, Schorry EK. *J Pediatr Orthop* 2006; 26: 413-23.
 14. Zamora AC, Collard HR, Wolters PJ, *et al.* Neurofibromatosis-associated lung disease: a case series and literature review. *Eur Respir J* 2007; 29: 210-4.
 15. Abe Y, Hatanaka H, Kamiya T, *et al.* Pulmonary sarcoma complicated with neurofibromatosis type 1 (NF1). *Anticancer Res* 2003; 23: 613-6.
 16. Tonsgard JH. Clinical manifestations and management of neurofibromatosis type 1. *Semin Pediatr Neurol* 2006; 13: 2-7.
 17. Preseton FW, Walsh WS, Clark TH. Cutaneous neurofibromatosis (von Recklinghausen's disease): clinical manifestations and incidence of sarcoma in 61 male patients. *Arch Surg* 1952; 64: 813-27.
 18. Zoller ME, Rembeck B, Oden A, *et al.* Malignant and benign tumors in patients with neurofibromatosis type 1 in a defined Swedish population *Cancer* 1997; 79: 2125-31.
 19. Hillier JC, Moskovic E. *Clin Radiol* 2005; 60: 960-7.
 20. Hutcherson RW, Jenkins HA, Canalis RF. Neurogenic sarcoma of the head and neck *Arch Otolaryngol* 1979; 105: 267-70.

成人第一型神經纖維瘤併發肺部惡性週邊神經鞘腫瘤轉移 ——病例報告

張晟瑜 吳振都* 林璟宏** 何肇基*** 楊泮池***

第一型神經纖維瘤或 von Recklinghausen's 疾病是一種自體顯性遺傳，發生率約三千分之一。惡性週邊神經鞘腫瘤（MPNST）是一種罕見的紡錘細胞肉瘤，由神經脊的 Schwann 細胞或生長細胞分化而來。有些惡性週邊神經鞘腫瘤跟第一型神經纖維瘤有相關。惡性週邊神經鞘腫瘤通常對化學及放射治療的反應不佳，尤其是那些第一型神經纖維瘤併發的惡性週邊神經鞘腫瘤。本文報告一例第一型神經纖維瘤病患，因併發肺部週邊神經鞘腫瘤轉移而導致呼吸衰竭，在接受化學治療後成功地脫離呼吸器。(*胸腔醫學* 2008; 23: 42-48)

關鍵詞：惡性週邊神經鞘腫瘤，第一型神經纖維瘤

Needlescopic Video-assisted Thoracic Surgery for Paraesophageal Bronchogenic Cyst

Jui-Ying Lee*, Yen-Lung Lee*, Hsien-Pin Li*, Shah-Hwa Chou*,** , Eing-Long Kao*,**

The authors report an adult with a paraesophageal bronchogenic cyst which was encountered incidentally during a routine chest roentgenogram in a health examination. Needlescopic video-assisted thoracic surgery was successfully utilized to remove the bronchogenic cyst that was densely adherent to the adjacent esophagus. After operation, the patient had an uneventful recovery and a normal esophagogram, and was discharged on postoperative day 4.

Our present case suggests that needlescopic video-assisted thoracic surgery provides a more minimally invasive technique with the same safety profile as conventional thoracoscopic surgery in managing mediastinal masses. (*Thorac Med* 2008; 23: 49-54)

Key words: needlescopic, VATS (video-assisted thoracic surgery), bronchogenic cyst

Introduction

Moutoux and associates first reported the excision of a bronchogenic cyst by video-assisted thoracoscopic surgery in 1991 [1]. With the technological development of needlescopic equipment and instruments, needlescopic video-assisted thoracic surgery has become more and more prevalent. Bronchogenic cysts of the mediastinum are uncommonly diagnosed in adults; therefore, surgical experience is limited, especially with regard to video-assisted thoracic surgery [2]. As a result, experience with needlescopic video-assisted thoracic surgery for removal of mediastinal bronchogenic cysts is rare. We herein present the case of a patient with a paraesophageal bronchogenic cyst, suspected on computed tomo-

graphy and confirmed by endoscopic ultrasound preoperatively. Surgical treatment for complete excision of the cyst with the successful application of the needlescopic technique was achieved. We would like to share our experience.

Case Report

A 26-year-old male, previously well, had a posterior mediastinal mass which was found incidentally on chest radiography (Figure 1) during pre-employment screening. Chest computed tomography (Figure 2) was done for further evaluation and demonstrated an iso-dense cystic lesion (3.2 x 3.0 x 4.4 cm) bulging to the left aspect of the posterior mediastinum. Differential diagnosis included a bronchogenic cyst, neuroen-

*Division of Thoracic Surgery, Department of Surgery, Kaohsiung Medical University Hospital, Kaohsiung, Taiwan,
**Department of Surgery, Faculty of Medical School, College of Medicine, Kaohsiung Medical University, Kaohsiung, Taiwan

Address reprint requests to: Dr. Eing-Long Kao, Division of Thoracic Surgery Department of Surgery, Kaohsiung Medical University Hospital, 100 Tzyou 1st Road, Kaohsiung 80708, Taiwan



Fig. 1. A mass in the left lower paraspinal region (black arrow)

teric cyst, and esophageal duplication cyst. To further define the intra-extramural extent of this cystic lesion, we arranged endoscopic ultrasound which revealed that the lesion was located outside the esophageal wall, at 30 cm to 37 cm from the upper incisors. Needlescopic thoracoscopy for exploration and complete excision of the cyst was planned.

Surgical Technique. Surgery was performed in the right lateral position under general anesthesia using double lumen. The left lung was collapsed. A 3-mm camera port was placed in the sixth intercostal space in the midaxillary line. Two 3-mm working ports were placed in the sixth and ninth intercostal space in the posterior axillary line (Figure 3). Using 3-mm thoracoscopy (Karl Storz GmbH & Co, Tuttlingen, Germany),

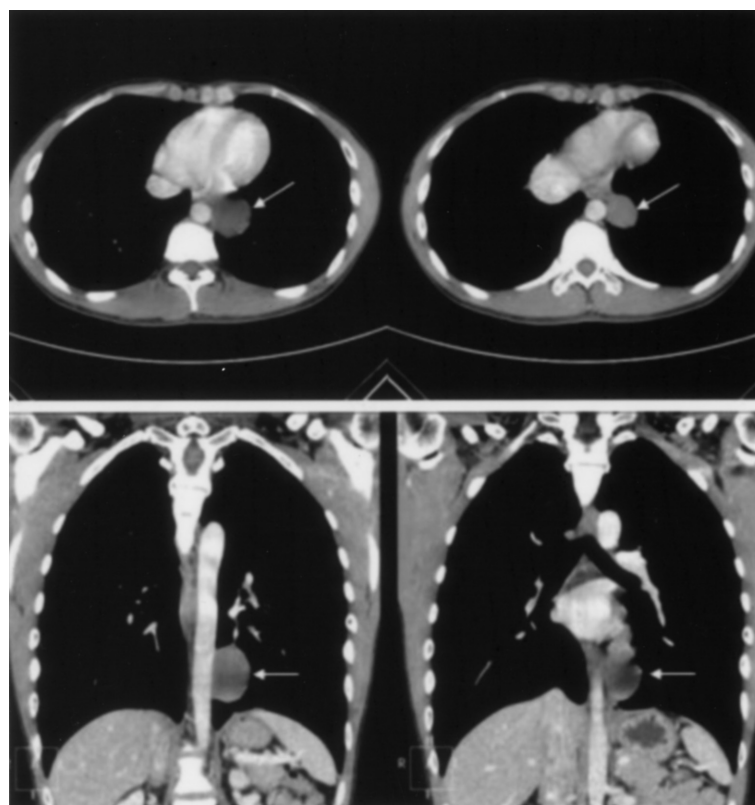


Fig. 2. Enhanced computed tomography of the lower thoracic level shows an ovoid, well-defined, non-enhanced and iso-dense (about 53 HU) cystic lesion sized 3.2 x 3.0 x 4.4 cm (white arrow) [The upper row: axial image; The lower row: coronal reformation]



Fig. 3. Note the incisions on the patient

the cystic wall that was adherent to the adjacent esophagus was dissected carefully using 3-mm hook-electrocautery. Since the muscular fibers of the esophagus were dissociated, we enlarged the wound and applied an endoGIA endoscopic linear stapler (United States Surgical Corporation, Norwalk, CT, USA) to divide the lesion from the esophagus, and sutured the defect of the muscular fibers at the same time. Operative time was approximately 100 minutes. At the completion of surgery, a nasogastric tube was used to insufflate the esophagus with air so as to exclude esophageal perforation. Before lung reexpansion, a 28 Fr chest tube was emplaced under direct vision via the enlarged port, which had been expanded for linear stapler passage and specimen extraction.

Postoperatively, the chest tube was removed

after a normal esophagogram on postoperative day 2, and the patient was discharged on postoperative day 4 with an uneventful recovery.

Histology showed variable-sized cystic spaces lined by cuboidal to columnar or attenuated ciliated epithelium and walled by inflamed stroma and bronchial glands. The pathologic diagnosis was compatible with bronchogenic cyst.

Discussion

Bronchogenic cysts, closed and epithelial-lined sacs, are thought to originate from the anomalous budding of the tracheal diverticulum from the primitive foregut between the third and sixth weeks of gestation [2-4]. Depending on the time of separation from the primary airways, the bronchogenic cyst may be either in the mediastinum or in the lungs as a result of anomalies in the fifth and sixth week of development, respectively [2, 4-5]. Bronchogenic cysts of the mediastinum are rare. In a series of 2,163 mediastinal lesions, 72 (3.3%) were found to be due to bronchogenic cysts [5].

Bronchogenic cyst frequently presents as an incidental radiological finding in adults, though some patients may have symptoms such as cough, purulent sputum, chest pain, dyspnea, dysphagia, dysphonia, anorexia, hemoptysis or weight loss [2, 6]. Rarely, life-threatening complications such as superior vena cava syndrome, tracheal compression or pneumothorax have been reported [6].

The management of mediastinal bronchogenic cysts includes observation, percutaneous or transbronchial aspiration, injection of sclerosing agents and total excision via thoracotomy, mediastinoscopy or thoracoscopy [7]. Nowadays, observation of the incidentally discovered lesions should not be encouraged, because with time they may become symptomatic and even a malignant

transformation [8-9]. Besides, intraoperative or postoperative complications such as bleeding or delayed bronchial rupture increase in symptomatic lesions [4, 7, 10]. Percutaneous or transbronchial aspiration, which is a relatively non-invasive intervention, has been proved to be both a diagnostically and therapeutically useful procedure. The utilization of endobronchial ultrasound allows us to make a real-time visualization for deep and complete transbronchial aspiration [11]. However, aspiration does not allow for the cystic lining removal that is the main cause of recurrence [11-12]. Therefore, complete surgical resection is advocated regardless of the presence or absence of symptoms [4, 6, 12-13].

Traditional surgical intervention is sternotomy or posteriolateral thoracotomy. Nevertheless, this causes significant postoperative pain and prolongs the duration of chest tube drainage and the hospital stay [7]. With the advances in endoscopic techniques and equipment, video-assisted thoracic surgery has been used with mediastinal masses since the early 1990s. Moutoux and associates first reported the excision of a bronchogenic cyst by video-assisted thoracoscopic surgery in 1991 [1]. Needleoscopic operations represent the next logical step in the evolution of video-assisted thoracic surgery, though needle-sized scopes (instruments with an external diameter of less than or equal to 3 mm) provide poor visibility. An accurate preoperative assessment is imperative for any successful thoracoscopic approach [2]. In the present case, chest computed tomography provided information on the relationship of the cyst and the adjacent structure. Endoscopic ultrasound, rather than esophagography, can clearly distinguish cystic from solid masses, as well as define the intra-extramural extent of lesions [14]. Consequently, we used the needlescopic technique in the removal of the asymptomatic paraesophageal bronchogenic cyst.

As the present case revealed, needlescopy also allowed precise visualization of the anatomy, and yielded satisfactory results and the same safety profile as conventional thoracoscopic surgery in managing mediastinal masses.

Acknowledgments

The authors thank Yu-Tang Chang, MD, for his insightful comments in reviewing the manuscript.

References

1. Mouroux J, Bourgeon A, Benchimol D, *et al.* Bronchogenic cysts of the esophagus. Classical surgery or video-surgery? *Chirurgie* 1991; 117: 564-8. [In French]
2. Weber T, Roth TC, Beshay M, *et al.* Video-assisted thoracoscopic surgery of mediastinal bronchogenic cysts in adults: A single-center experience. *Ann Thorac Surg* 2004; 78: 987-91.
3. Wychulis AR, Payne WS, Clagett OT, *et al.* Surgical treatment of mediastinal tumors. *J Thorac Cardiovasc Surg* 1971; 62: 379-92.
4. St-Georges R, Deslauriers J, Duranceau A, *et al.* Clinical spectrum of bronchogenic cysts of the mediastinum and lung in the adult. *Ann Thorac Surg* 1991; 52: 6-13.
5. Lysterly HK, Sabiston DC Jr. Primary neoplasms and cysts of the mediastinum. In: Fishman AP, ed. *Pulmonary Diseases and Disorders*. Vol. 3, 2nd ed. New York: McGraw-Hill, 1988: 2090-105.
6. Aktou S, Yuncu G, Halilcolar H, *et al.* Bronchogenic cysts: clinicopathological presentation and treatment. *Eur Resp J* 1996; 9: 2017-21.
7. Martinod E, Pons F, Azorin J, *et al.* Thoracoscopic excision of mediastinal bronchogenic cysts: results in 20 cases. *Ann Thorac Surg* 2000; 69: 1525-8.
8. Lozano MF, Gonzales-Martinez B, More LS, *et al.* Carcinoma arising in a calcified bronchogenic cyst. *Respiration* 1981; 42: 135-7.
9. Okada Y, Mori H, Maeda T, *et al.* Congenital mediastinal bronchogenic cyst with malignant transformation: an

- autopsy report. *Pathol Int* 1996; 46: 594-600.
10. Cho DG, Kwack MS Video-assisted thoracoscopic closure of the delayed bronchial rupture after thoracoscopic resection of mediastinal bronchogenic cyst. *Chest* 1999; 115: 257-9.
 11. Galluccio G, Lucantoni G. Mediastinal bronchogenic cyst's recurrence treated with EBUS-FNA with a long-term follow-up. *Eur J Cardiothorac Surg* 2006; 29: 627-9; discussion 629.
 12. Suen HC, Mathisen DJ, Grillo HC, *et al.* Surgical management and radiological characteristics of bronchogenic cysts. *Ann Thorac Surg* 1993; 55: 476-81.
 13. Patel SR, Meeker DP, Biscotti CV, *et al.* Presentation and management of bronchogenic cysts in the adult. *Chest* 1994; 106: 79-85.
 14. Lim LL, Ho KY, Goh PM. Preoperative diagnosis of a paraesophageal bronchogenic cyst using endosonography. *Ann Thorac Surg* 2002; 73: 633-5.

迷你胸腔鏡手術應用於食道旁支氣管源性囊腫的切除

李瑞英* 李彥龍* 李憲斌* 周世華*,** 高英隆*,**

縱膈腔支氣管源性囊腫並不常見於成人，因此以胸腔鏡來處理這類囊腫的經驗可以說是相當難得；隨著微創手術的概念以及內視鏡手術技術與器械的進步，迷你胸腔鏡手術開始被應用於各種胸腔手術之中。

我們在此分享一個成功應用迷你胸腔鏡手術完整移除和食道壁緊黏的支氣管源性囊腫之經驗。這個二十六歲沒有任何系統性疾病的男性，在一次例行性健康檢查之中意外發現食道旁支氣管源性囊腫的存在，經過胸部電腦斷層以及內視鏡超音波的評估之後，我們決定以迷你胸腔鏡手術為病人切除病灶；術後第二天病人在食道攝影確認無滲漏後順利移除胸管，並於術後第四天出院。

這個經驗告訴我們，在謹慎的術前評估之後，即使迷你胸腔鏡的視野較小，其應用於縱膈腔腫瘤的切除，相較於傳統胸腔鏡手術，在安全上並無二致；而迷你胸腔鏡手術因傷口更小，可以減輕病人術後的疼痛感，縮短病人的胸管引流時間以及住院天數，並增加病患對傷口美觀的滿意度。(*胸腔醫學* 2008; 23: 49-54)

關鍵詞：迷你胸腔鏡，胸腔鏡手術，支氣管源性囊腫

* 高雄醫學大學附設中和紀念醫院 外科部胸腔外科，** 高雄醫學大學醫學院 醫學系外科學

索取抽印本請聯絡：高英隆醫師，高雄醫學大學附設中和紀念醫院 外科部胸腔外科，高雄市三民區自由一路 100 號

Hemophagocytic Syndrome Associated with Diffuse Large B-Cell Lymphoma: A Case Report

Chih-Hsiung Chen, Kun-Ming Chung*, Jiunn-Min Shieh, Shian-Chin Ko,
Hsiu-Nien Shen*, Kuo-Chen Cheng*

A 54-year-old woman was admitted to Chi-Mei Foundation Hospital because of fever, chills and left lower chest pain. The laboratory findings revealed bicytopenia (anemia and thrombocytopenia), an abnormal liver profile, and elevated blood levels of C-reactive protein, ferritin and triglyceride. She was endotracheally intubated and received mechanical ventilation due to respiratory distress. Hepatosplenomegaly was found in her abdominal computed tomographic scan. Bone marrow biopsy revealed active hemophagocytosis. Because of the prolonged febrile state, a gallium scan was performed, which revealed neck and mediastinal lymphadenopathy. The neck lymph node biopsy was proven to be diffuse large B-cell lymphoma (DLBCL). A diagnosis of DLBCL associated with hemophagocytic syndrome (HPS) was made. However, uncontrolled sepsis developed after chemotherapy with cyclophosphamide, oncovorin, and dexamethasone, and the patient died. DLBCL associated with HPS is rare and has been effectively treated with chemotherapy in some reports. The safety of chemotherapy for DLBCL-related HPS has never been reported in critically ill patients with mechanical ventilation, and the prognosis is extremely poor. (*Thorac Med* 2008; 23: 55-60)

Key words: Hemophagocytic syndrome, diffuse large B-cell lymphoma

Introduction

Hemophagocytic syndrome (HPS) is the phenomenon in which activated macrophages phagocytize red blood cells, white blood cells, and platelets. It is characterized by febrile pancytopenia, jaundice, hepatosplenomegaly, and hemophagocytosis in the bone marrow, liver, or lymph nodes [1]. A variety of infectious diseases, including viral, bacterial, fungal, and parasitic infections [2-4], collagen-vascular diseases, and

malignancies, are associated with HPS. HPS has also been associated with almost all T-cell lymphomas [5-7]; this phenomenon is less common in B-cell lymphomas. In this study, we report a diffuse large B-cell lymphoma associated with reactive hemophagocytosis.

Case Report

A 54-year-old woman was admitted to Chi-Mei Foundation Hospital because of fever, chills

Division of Chest Medicine, Department of Internal Medicine; *Department of Critical Care Medicine; Chi Mei Foundation Medical Center, Tainan

Address reprint requests to: Dr. Hsiu-Nien Shen, Department of Critical Care Medicine, Chi Mei Foundation Medical Center, 901 Chung-Hwa Road, Yung Kang City, Tainan 710, Taiwan, R.O.C.

and left lower chest pain. The laboratory findings on admission revealed bicytopenia (hemoglobin 6.9 g/dL, platelets 43,000/mL), a higher C-reactive protein level (358 mg/L), and an abnormal liver profile (aspartate aminotransferase 105 U/L, alanine aminotransferase 20 U/L, gamma-glutamyl transferase 210 U/L, total bilirubin 7.09 mg/dL, direct bilirubin 6.57 mg/dL). She was endotracheally intubated and mechanically ventilated because of acute respiratory failure. Due to a suspicion of intraabdominal infection, an abdominal computed tomographic (CT) scan was done, which depicted only hepatosplenomegaly. There was no intraabdominal abscess, and no biliary stones. She was treated with antibiotics after blood, sputum, and urine cultures were obtained.

A hematologist was consulted. The blood sample was drawn, and hyperferritinemia ($> 2,000$ ng/mL) and hypertriglyceridemia (241 mg/dL) were noted. A bone marrow examination from the iliac crest was performed, and the specimens revealed activated histiocytes phagocytizing red blood cells, consistent with hemophagocytic syndrome (Figure 1). A gallium scan revealed multiple neck and mediastinal lymphadenopathies (Figure 2). The chest CT also confirmed the existence of numerous lymphadenopathies at the bilateral neck (Figure 3), supraclavicular region, bilateral axilla, mediastinum, and retroperitoneum.

On physical examination, palpable stony hard lymph nodes around the bilateral supraclavicular fossa and neck were found. After percutaneous lymphadenectomy, biopsy showed diffused lymphoid infiltrates with infarction and coagulative necrosis. Immunohistochemically, these atypical lymphocytes expressed CD20 (Figure 4), Bcl-2, Bcl-6, MUM-1, and IgM without CD3, CD10, CD30, IgD, HHV-8-LANA, and EBV-LMP-1.

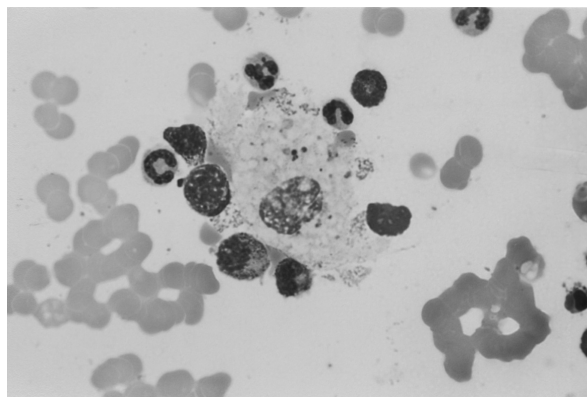


Fig. 1. Three red blood cells in the cytoplasm and 2 attached to the membrane of the activated histiocyte, consistent with hemophagocytosis, found in the iliac crest marrow biopsy (original magnification $\times 1000$).

The CD21 staining highlighted focal residual follicular dendritic meshworks. The proliferation fraction as determined by Ki-67 was high at 90%. A diagnosis of diffuse large B-cell lymphoma (DLBCL) associated with hemophagocytic syndrome (HPS) was made.

The oncologists suggested cyclophosphamide, oncovorin, and dexamethasone as chemotherapy agents. After receiving chemotherapy, pancytopenia developed (leukocyte count 200/mL with an absolute granulocyte count of 168/mL, hemoglobin 5.3 g/dL, and platelet count of 5000/mL). Her later hospitalization course was complicated by refractory metabolic acidosis (pH 7.318, $p\text{CO}_2$ 23.9 mmHg, HCO_3^- 12.0 mmHg, base excess -12.0 mmHg), and acute renal failure (creatinine 3.3 mg/dL, compared with the previous level of 0.6 mg/dL within 10 days). The patient died of uncontrolled sepsis after futile antibiotics therapy.

Discussion

HPS is associated with various conditions, such as viral, bacterial, fungal, and parasitic infec-

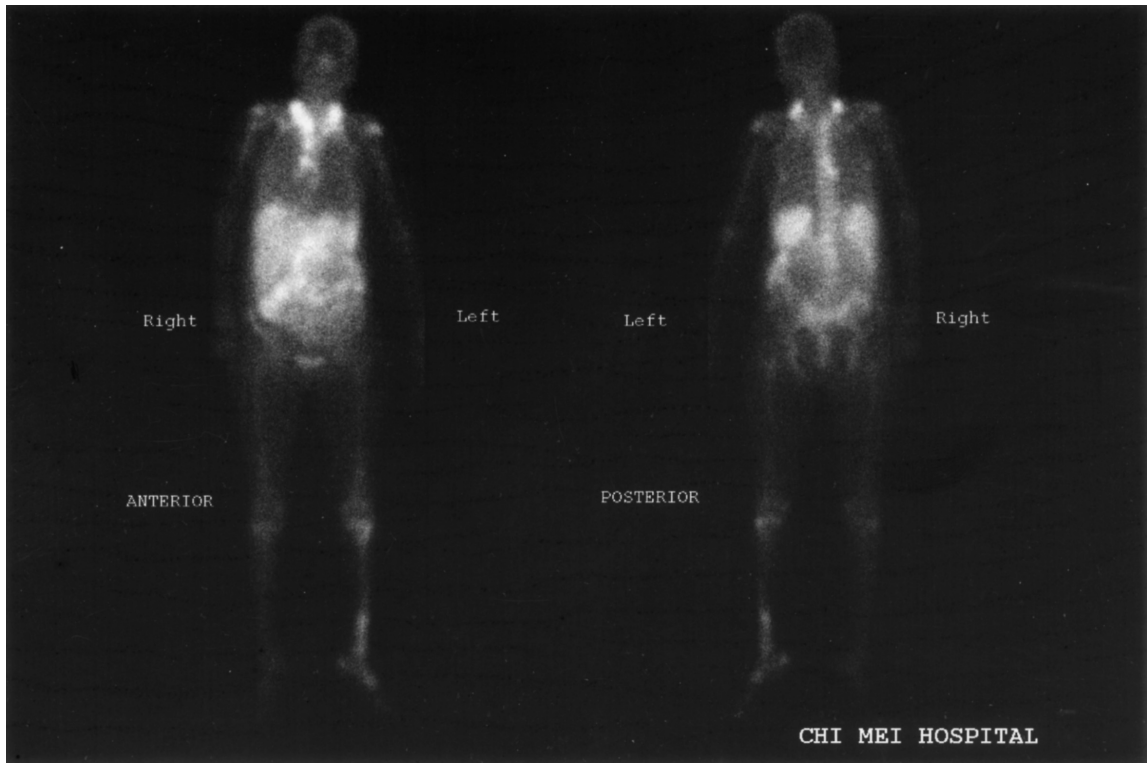


Fig. 2. Gallium scan showing multiple neck and mediastinal lymphadenopathy.

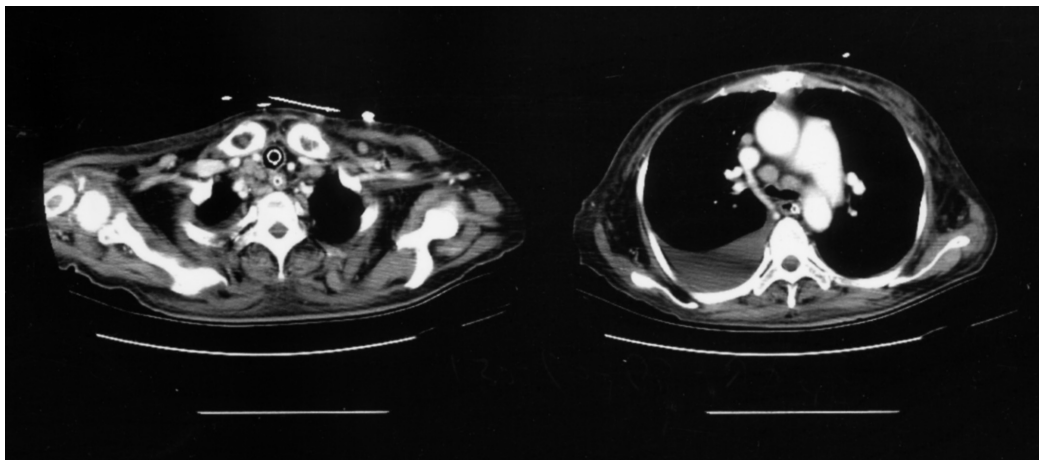


Fig. 3. Numerous lymphadenopathies at the bilateral neck and subcarinal area, found in the chest CT.

tious diseases [2-4], collagen-vascular diseases, and hemato-oncologic cancers. An analysis of 23 patients with HPS in Taiwan disclosed that most HPS cases are related to hematologic malignancies, including non-Hodgkin's lymphomas,

leukemia, and myelodysplastic syndromes. Non-Hodgkin's lymphomas were the major cause, and only 2 B-cell lymphomas were found in an etiology study [7]. A series with a small number of cases in 1975 also confirmed T-lymphoma

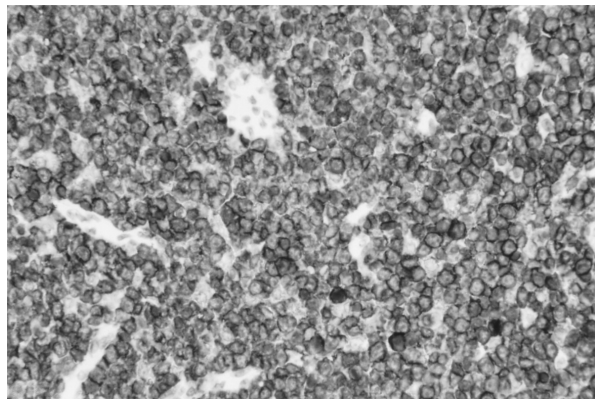


Fig. 4. Atypical lymphocytes expressing CD20 immunohistochemically (original magnification $\times 400$).

predominance [5]. HPS was once considered only to be associated with T-cell type lymphomas and in all types of histology [5-7]. HPS does occur in B-cell lymphoma, though much less commonly, and when it does, it is called B-cell lymphoma-associated HPS (BCL-HPS).

BCL-HPS has several special clinical features. It is most often reported in Japanese populations in the medical literature [8], and even though lymphoma resulting in hemophagocytosis has T-lymphoma predominance, the predominance is not observed in Japanese populations [9]. Murase *et al.* proposed an Asian variant of intravascular lymphomatosis, called malignant histiocytosis-like B-cell lymphoma [10]. The cause of the racial difference remains unclear, and requires further investigation.

In a reassessment of previously reported cases in 1975, Wilson reported the earliest BCL-HPS [5]. However, the paper does not describe which histology of B-cell lymphoma caused HPS. In 1992, Barberan reported a fulminant and rapidly fatal case of HPS related to kappa-monoclonal B immunoblastic lymphoma [11]. Other case reports include T-cell-rich B-cell lymphoma [12], angiotropic B-cell lymphoma [13], and diffuse large B-cell lymphoma [14-15]. All these patients had

a fulminant course, complicated by febrile pancytopenia, and died of severe sepsis [11-15].

The most common manifestations of lymphoma-related HPS are swinging fever and peripheral blood cytopenia [16]. Peripheral lymphadenopathy is not always found in these cases. The absence of peripheral lymphadenopathy makes the diagnosis of BCL-HPS difficult, especially if there are no bone marrow infiltrations [17]. Since BCL-HPS is characterized by a fulminant course and rapid fatality, the patients affected by BCL-HPS are diagnosed after autopsy [11-14].

In general, HPS is considered to be a cytokine dysregulation resulting in histiocyte activation. Non-specific management for HPS is immunosuppressive drugs with methylprednisolone or cytotoxic agents such as cyclosporine. Because different diseases cause HPS, the underlying conditions should be considered to begin definite therapy. If the HPS is caused by infection, adequate anti-microbial agents are considered reasonable [2-4]. Any administration of immunosuppressive or cytotoxic agents is contraindicated in these conditions. In collagen-vascular disease-related HPS, for example systemic lupus erythematosus, methylprednisolone alone or with intravenous immunoglobulin is effective in some cases [18]. The therapy should be started after a detailed etiology workup, if possible, and aimed toward treating the underlying disease, in order to achieving the best outcome.

Chemotherapy is effective in controlling lymphoma. For BCL-HPS, chemotherapeutic agents with cyclophosphamide, adriamycin, vincristine, and prednisolone (CHOP) were the acceptable regimen in previous reports [15, 19-20], and achieved a successful resolution in 1 patient [15]. However, another case report showed a higher recurrence rate of B-cell lymphoma after chemotherapy, even during the interval after chemo-

therapy [19].

Our patient was admitted because of pancytopenic fever. Although HPS was diagnosed after serial blood biochemistry workup, the underlying disease itself was diagnosed after the presence of a neck lymph node. Because of the diagnostic difficulty reported previously, BCL-HPS should be considered, and a whole body gallium scan is indicated due to the possibility of the absence of a peripheral lymph node. However, with an acceptable CHOP regimen for the condition, the prognosis remained unclear. In patients with mechanical ventilation, the outcome is extremely poor.

References

1. Chan JK, Ng CS, Law CK, *et al.* Reactive hemophagocytic syndrome: a study of 7 fatal cases. *Pathology* 1987; 19: 43-50.
2. Risdall RJ, McKenna RW, Nesbit ME, *et al.* Virus-associated hemophagocytic syndrome: a benign histiocytic proliferation distinct from malignant histiocytosis. *Cancer* 1979; 44: 993-1002.
3. Cohen RA, Hutter JJ, Boxer MA, *et al.* Histiocytic medullary reticulosis associated with acute Epstein-Barr (EB) virus infection. *Am J Pediatr Hematol Oncol* 1980; 2: 245-8.
4. Risdall RJ, Brunning RD, Hernandez JJ, *et al.* Bacteria-associated hemophagocytic syndrome. *Cancer* 1984; 54: 2968-72.
5. Wilson MS, Weiss LM, Gatter KC, *et al.* Malignant histiocytosis. A reassessment of cases previously reported in 1975 based on paraffin section immunophenotyping studies. *Cancer* 1990; 66: 530-6.
6. Liang DC, Chu ML, Shih CC. Reactive histiocytosis in acute lymphoblastic leukemia and non-Hodgkin's lymphoma. *Cancer* 1986; 58: 1289-94.
7. Chang CS, Wang CH, Su IJ, *et al.* Hematophagic histiocytosis: a clinicopathologic analysis of 23 cases with special reference to the association with peripheral T-cell lymphoma. *J Formos Med Assoc* 1994; 93: 421-8.
8. Shimazaki C, Inaba T, Nakagawa M. B-cell lymphoma-associated hemophagocytic syndrome. *Leuk Lymphoma* 2000; 38: 121-30.
9. Takahashi N, Chubachi A, Miura I, *et al.* Lymphoma-associated hemophagocytic syndrome in Japan. *Rinsho Ketsueki* 1999; 40: 542-9.
10. Murase T, Nakamura S. An Asian variant of intravascular lymphomatosis: an updated review of malignant histiocytosis-like B-cell lymphoma. *Leuk Lymphoma* 1999; 33: 459-73.
11. Barberan J, Pastor JM, Menendez MA, *et al.* The reactive hemophagocytic syndrome associated with immunoblastic B-cell lymphoma. *Rev Clin Esp* 1992; 190: 308-10.
12. Dommann-Scherrer C, Zimmermann D, Hassam S, *et al.* T-cell rich B-cell lymphoma associated with hemophagocytic syndrome. *Verh Dtsch Ges Pathol* 1992; 76: 122-5.
13. Okada Y, Nakanishi I, Nomura H, *et al.* Angiotropic B-cell lymphoma with hemophagocytic syndrome. *Pathol Res Pract* 1994; 190: 718-24.
14. Yamada K, Katoh K, Okuyama M. Diffuse B-cell lymphoma associated with hemophagocytic syndrome. *Rinsho Ketsueki* 1996; 37: 161-4.
15. Suzuki T, Nonaka Y, Hayashi T, *et al.* Diffuse B-cell lymphoma associated with hemophagocytic syndrome. *Rinsho Ketsueki* 1998; 39: 59-65.
16. Wong KF, Chan JK, Ng CS, *et al.* Large cell lymphoma with initial presentation in the bone marrow. *Hematol Oncol* 1992; 10: 261-71.
17. Buchi G, Termine G, Orlassino R, *et al.* Hemophagocytic syndrome in a case of splenic large B-cell lymphoma. *Tumori* 1996; 82: 621-4.
18. Qian J, Yang CD. Hemophagocytic syndrome as one of main manifestations in untreated systemic lupus erythematosus: two case reports and literature review. *Clin Rheumatol* 2006.
19. Motegi S, Nishizaki Y, Muramatsu C, *et al.* Hemophagocytic syndrome in ileum-origin B-cell lymphoma. *J Gastroenterol* 2003; 38: 995-9.
20. Anghel G, Petrinato G, Severino A, *et al.* Intravascular B-cell lymphoma: report of two cases with different clinical presentation but rapid central nervous system involvement. *Leuk Lymphoma* 2003; 44: 1353-9.

瀰漫性大 B 細胞淋巴瘤引起的嗜血症候群：病例報告

陳志雄 鍾焜明* 謝俊民 柯獻欽 沈修年* 鄭高珍*

一名 54 歲女性因為發燒、寒顫以及左下胸痛而住院。實驗室檢查顯示紅血球以及血小板兩種血球減少、不正常的肝指數、以及升高的 C 反應蛋白、血中儲鐵蛋白和三酸甘油脂。因為呼吸困難，病人在插入氣管內管後接受機器通氣治療。她的腹部電腦斷層顯示肝脾腫大，骨髓穿刺切片顯現活動中的血細胞吞噬情形。因為持續的發燒，在接受鎂 67 造影掃描後顯示明顯變大的頸部和縱膈淋巴結，頸部淋巴結組織切片證實為瀰漫性大 B 細胞淋巴瘤，病人因此診斷瀰漫性大 B 細胞淋巴瘤引起的嗜血症候群。在接受 cyclophosphamide、oncovirin、和 dexamethasone 為主的化學治療後，病人出現無法控制的敗血症而死亡。由 B 細胞淋巴瘤造成的嗜血症候群是十分罕見的；此外，雖然某些個案報告提出嗜血症候群可以使用化學治療來有效控制，但對於接受機器通氣之重症病人的化學治療安全性從來沒有被提出來過。基于本病例個案，我們認為在機器通氣的重症病人使用化學治療來控制瀰漫性大 B 細胞淋巴瘤引起的嗜血症候群的預後是不佳的。(胸腔醫學 2008; 23: 55-60)

關鍵詞：嗜血症候群，瀰漫性大 B 細胞淋巴瘤

Atypical Presentation of Hepatic Epithelioid Hemangioendothelioma as a Pulmonary Mass Lesion on Chest Radiograph: A Case Report

Sheng-Yao Yu, Fung-J Lin, Chi-Yuan Tzen*, Chien-Liang Wu

Epithelioid hemangioendothelioma is a rare tumor. It can originate from many organs, including the liver, lung, and soft tissue. We describe a patient with hepatic epithelioid hemangioendothelioma presenting as a pulmonary mass lesion on chest radiograph. There has been no such presentation previously. We also discuss the thoracic imaging characteristics of epithelioid hemangioendothelioma in the present case report. (*Thorac Med* 2008; 23: 61-65)

Key words: epithelioid hemangioendothelioma

Introduction

Epithelioid hemangioendothelioma (EHE) is a rare tumor of vascular origin, it can originate from many organs, including the liver, lung and soft tissue. Different organs have different presentations on imaging. This report describes atypical presentation of hepatic EHE mimicking lung tumor on chest radiograph.

Case Report

A 72-year-old male ex-smoker presented with a 2-month history of hoarseness. He also had cough with scanty sputum for 2 weeks and intermittent fever for 1 week. He denied any abdominal discomfort. On physical examination, there was no remarkable finding except right upper quadrant tenderness. His white blood cell

count was 11,900/uL with a shift to the left, and hemoglobin 9.7 g/dL. Other laboratory studies showed elevated alkaline phosphatase of 311 IU/L (normal, 40-120 IU/L), aspartate aminotransferase 41 IU/L (normal, 5-35 IU/L), alanine aminotransferase 37 IU/L (normal, 5-30 IU/L), total bilirubin 1.5 mg/dL (normal, 0.2-1.3 mg/dL), and direct bilirubin 0.8 mg/dL (normal, 0-0.4 mg/dL). The chest radiograph showed an ill-defined mass at the right lower lung field near the heart border (Figure 1). The initial impression was a lung tumor, but computed tomographic (CT) scanning of the thorax suggested a huge liver tumor with marginal enhancement and central necrosis near the dome (Figure 2). The liver tumor protruded into the pleural cavity with a clear interface to the lung. Cancer antigen 19-9 (CA 19-9) was 23.43 U/ml (normal, < 30.00 U/ml), and the carcinoembryonic antigen (CEA)

Division of Chest Medicine, Department of Internal Medicine, Mackay Memorial Hospital, Taipei, Taiwan; *Department of Pathology, Mackay Memorial Hospital, Taipei, Taiwan

Address reprint requests to: Dr. Fung-J Lin, Division of Chest Medicine, Department of Internal Medicine, Mackay Memorial Hospital, Taipei, Taiwan, 92, Section 2, Chung-shan North Road, Taipei, Taiwan

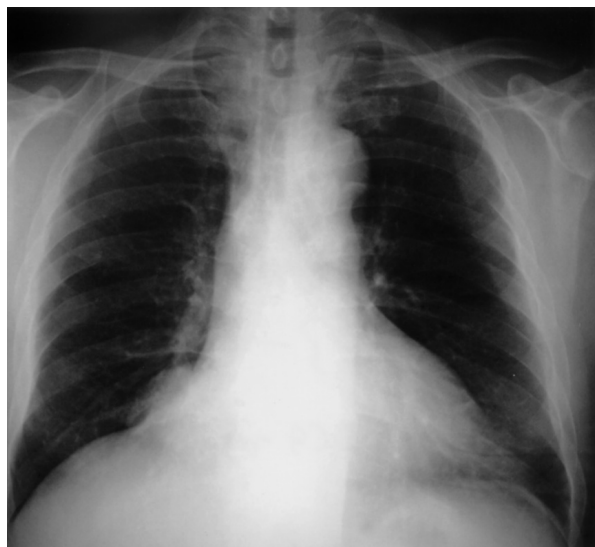
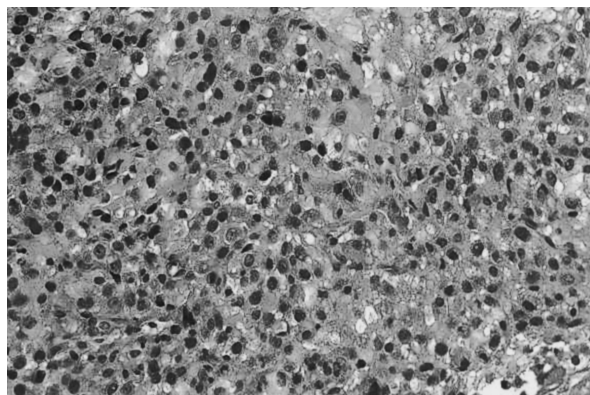


Fig. 1. Chest radiograph shows an ill-defined mass at the right lower lung field near the heart border.

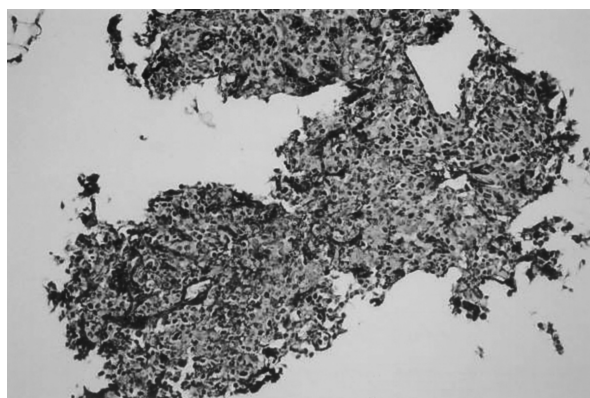


Fig. 2. Chest tomography scan showing a huge liver tumor with marginal enhancement and central necrosis.

level was 0.85 ng/ml (normal, < 5.00 ng/ml). Specimens by fine needle aspiration showed a tumor composed of sheets of epithelioid cells possessing abundant eosinophilic cytoplasm. Immunohistochemically, the tumor cells were positive for Factor VIII-related antigen (von Willebrand



(A)



(B)

Fig. 3. Micrography shows soft tissue involved in a tumor composed of sheets of epithelioid cells possessing abundant eosinophilic cytoplasm (Penal A). Immunohistochemically, the tumor is diffusely positive for vimentin, and partially positive for factor VIII-related antigen (von Willebrand factor) (Panel B).

factor) (Figure 3), and totally negative for cytokeratins, thyroid transcription factor-1, and alpha-fetoprotein. The pathologic diagnosis was hepatic EHE.

Because of his poor performance status, the patient was treated with the best supportive therapy. He died of multiple organ failure 2 months after diagnosis.

Discussion

EHE is a rare neoplasm of vascular origin.

The first recognition of this tumor was by Dail and Liebow in 1975 [1]. They described a similar tumor known as an intravascular bronchioloalveolar tumor. Using immunohistochemical techniques, Corrin and coworkers found the tumor cells were from a lineage capable of differentiation along endothelial lines [2]. Weiss and Enzinger were the first to offer the term “epithelioid hemangioendothelioma” (EHE) in 1982 [3]. Ishak and coworkers described primary involvement of EHE in the liver in 1984 [4]. This tumor is a low-grade malignancy, and can arise from many organ systems, including the liver, lung, pleura, bone, brain, thyroid gland, and soft tissues. Liver involvement could be metastatic or primary [5].

The symptoms of our patient were consistent with lung disease, and it was rational to consider the tumor was bronchogenic. Surprisingly, CT scanning revealed the tumor was in the liver, with a clear border at the lung. In fact, the possible origin of the tumor in our patient could include the liver, diaphragm, pleura or the lung, but interestingly, the patient’s manifestations were atypical of any possible source.

The features of pulmonary EHE on CT scan [6-7] were the presence of multiple perivascular nodules with well- or ill-defined margins with or without pleural effusion. Ground glass opacity was also reported. Most patients with pulmonary EHE were asymptomatic or had only mild cough and dyspnea. The tumor was usually found incidentally [6].

The pleura is another possible origin. Most patients with pleural EHE had chest pain or dyspnea [8]; this was not complained by our patient. Pleural EHE showed smooth or nodular pleural thickening with pleural effusion [8]. Our patient had no pleural effusion.

The diaphragm is also a possible origin.

There was only 1 case report of diaphragmatic EHE in the literature. That patient had pleural effusion and the tumor was a complex mass with cystic components contiguous with the diaphragm [9].

Although our patient did not complain of abdominal discomfort, he had right upper quadrant tenderness on physical examination; this is the most common symptom of patients with hepatic EHE. Other symptoms of hepatic EHE include weight loss, jaundice, fever, and fatigability [10-11]. Increased concentrations of serum alkaline phosphatase and aspartate aminotransferase, and alanine aminotransferase were also described [10-11]. Serum α -fetoprotein was raised in only 2.7% of the patients, while the concentrations of CEA and CA19-9 were not increased [10-11]. However, the presentation of our patient on CT scanning was atypical. The classic features of hepatic EHE on CT scanning [10] are of 2 different types – nodular and diffuse. The nodular type, as an early manifestation of the disease, reveals multiple hypodense nodular lesions, and can affect both lobes. The diffuse type, as a later stage of the disease, originates from the nodular type, with the lesions increasing in size and finally coalescing, forming extensive peripheral lesions. Focal calcification within the tumor is not an uncommon finding. However, there has been no report of hepatic EHE not only invading the liver capsule, and the diaphragm, but also protruding into the pleural cavity.

EHE causes diagnostic difficulty in pathology because of the pleomorphism of the tumor cells together with the varied patterns of the tumors and the various parenchymal and stromal reactions. The key to the diagnosis was the demonstration of cells containing Factor VIII related-antigen [10]. It is difficult to diagnose such a rare tumor based on specimens from fine needle

aspiration. Lauffer *et al.* suggested that only laparotomy and open biopsy could help to establish the correct diagnosis, and fine needle aspiration should not be performed due to possible bleeding [10]. However, Makhlouf *et al.* reviewed 137 patients with hepatic EHE, and the diagnosis was made by percutaneous needle biopsy specimens in 30 cases (22%) [11]. In addition, Cronin and Arenberg suggested the diagnosis of pulmonary EHE could be made by transbronchial biopsy [6]. The pathologic findings of our patient were consistent with the classic features of EHE, including a positive test for Factor VIII-related antigen immunohistochemically.

Conclusion

Hepatic EHE is a rare tumor. We described a case with an atypical presentation of a lung tumor on chest radiograph. The diagnosis was confirmed by immunohistochemical techniques, in which the tumor cells were positive for Factor VIII-related antigen.

References

1. Dail DH, Liebow AA, Gmelich JT, *et al.* Intravascular, bronchiolar and alveolar tumor of the lung (IVBAT). *Cancer* 1983; 51: 452-64.
2. Corrin B, Manners B, Millard M, *et al.* Histogenesis of the so-called intravascular bronchioloalveolar tumour. *J Pathol* 1979; 128: 163-7.
3. Weiss SW, Enzinger FM. Epithelioid hemangioendothelioma: a vascular tumor often mistaken for a carcinoma. *Cancer* 1982; 50: 970-81.
4. Ishak KG, Sesterhenn IA, Goodman MZD, *et al.* Epithelioid hemangioendothelioma of the liver: a clinicopathologic and follow-up study of 32 cases. *Hum Pathol* 1984; 15: 839-52.
5. Lerut JP, Orlando G, Sempoux C, *et al.* Hepatic haemangioendothelioma in adults: excellent outcome following liver transplantation. *Transpl Int* 2004; 17: 202-7.
6. Cronin P, Arenberg D. Pulmonary epithelioid hemangioendothelioma: an unusual case and a review of the literature. *Chest* 2004; 125: 789-92.
7. Sakamoto N, Adachi S, Monzawa S, *et al.* High resolution CT findings of pulmonary epithelioid hemangioendothelioma: unusual manifestations in 2 cases. *J Thorac Imaging* 2005; 20: 236-8.
8. Crotty EJ, McAdams HP, Erasmus JJ, *et al.* Epithelioid hemangioendothelioma of the pleura: clinical and radiologic features. *AJR* 2000; 175: 1545-9.
9. Bevelacqua FA, Valensi Q, Hulnick D. Epithelioid hemangioendothelioma. A rare tumor with variable prognosis presenting as a pleural effusion. *Chest* 1988; 93: 665-6.
10. Lauffer JM, Zimmermann A, Krähenbühl L, *et al.* Epithelioid hemangioendothelioma of the liver: A rare hepatic tumor. *Cancer* 1996; 78: 2318-27.
11. Makhlouf HR, Ishak KG, Goodman ZD. Epithelioid hemangioendothelioma of the liver: A clinicopathologic study of 137 cases. *Cancer* 1998; 85: 562-82.

肝臟類上皮性血管內皮瘤以肺部腫塊的不典型表現 —病例報告

游勝耀 林芳杰 曾岐元* 吳健樑

類上皮性血管內皮瘤是一種少見的腫瘤。它可以源自許多種器官，包括肝臟，肺臟，及軟組織。我們報告了一位肝臟類上皮性血管內皮瘤的患者的腫瘤在胸部影像檢查上像是肺部腫瘤的不典型表現。以前並未有類似的報告。我們也討論胸部類上皮性血管內皮瘤在影像學表現的特徵。(胸腔醫學 2008; 23: 61-65)

關鍵詞：類上皮性血管內皮瘤

Endobronchial Ultrasonography (EBUS) to Differentiate Tuberculoma from Lung Cancer — A Case Report and Literature Review

Tsai-Yu Wang, Chih-Hsi Kuo, Hao-Cheng Chen, Ren-Chin Wu*, Chien-Ying Liu

The coexistence of lung cancer and pulmonary tuberculosis is not uncommon in Taiwan, so determining the nature of a lung mass is critically important for physicians, in order to reach a definite diagnosis and therapy. The diagnostic yield of the peripheral lung abnormality using bronchoscopy alone is limited; however, the development of miniature probes and endobronchial ultrasonography (EBUS) has improved the accurate localization of peripheral lung lesions and the diagnostic rates. Furthermore, EBUS images are also helpful in differentiating between benign and malignant lung abnormalities. EBUS detected a heterogeneous mass with continuous hyperechoic margin in the right middle lobe and another mass with hyperechoic dots and discontinuous hyperechoic margin in the left upper lobe of a 67-year-old man with coexisting lung adenocarcinoma and pulmonary tuberculoma, who presented 2 lung masses in different lobes. The 2 image patterns suggested malignant versus benign lung abnormalities of the 2 masses, respectively, which were confirmed by the pathologic and bacteriologic studies. The literature concerning the coexistence of lung cancer and tuberculosis and the imaging characteristics of EBUS in lung abnormalities are reviewed. (*Thorac Med* 2008; 23: 66-72)

Key words: endobronchial ultrasonography (EBUS), tuberculosis (TB), lung cancer

Introduction

Lung cancer is prevalent and is the leading cause of cancer mortality in Taiwan, where pulmonary tuberculosis still remains an endemic disease. A study by Tamura *et al.* has shown that the incidence of lung cancer among patients with active pulmonary tuberculosis has increased, and vice versa [1]. Therefore, it is critically important to determine the nature of a pulmonary nodule or mass to reach a definite diagnosis and begin

treatment. Bronchoscopy has been used for evaluating pulmonary nodules, but it is still a challenge to approach peripheral lung nodules using this method, with its diagnostic accuracy ranging from 17% to 66% [2]. Recent advances in the technique of endobronchial ultrasonography (EBUS) have brought the advantage of increased accuracy to the diagnosis of peripheral lung nodules [3]. In addition to facilitating the accurate localization of the peripheral lung lesions [4-5], the imaging characteristics of

Department of Thoracic Medicine, and * Department of Pathology, Chang Gung Memorial Hospital, and School of Medicine, Chang Gung University, Taipei, Taiwan

Address reprint requests to: Dr. Chien-Ying Liu, Department of Thoracic Medicine, Chang Gung Memorial Hospital, 199, Tun-Hwa N. Rd., Taipei 105, Taiwan

EBUS also provide vital information useful in determining the nature of lung abnormalities [6-9].

We herein report a case with a lung mass in the right middle lobe (RML) and another lung nodule in the left upper lobe (LUL), detected on the chest radiograph and computed tomograph, but without a visible endobronchial tumor on bronchoscopy or other anatomic lesions on cancer screening. EBUS was used during bronchoscopy to localize the lesions for bronchoalveolar lavage (BAL) and transbronchial biopsy (TBB). The differential imaging characteristics of the 2 lesions were also detected. A lung adenocarcinoma (RML) with pulmonary tuberculosis (LUL) was finally diagnosed by means of the characteristic EBUS features, *Mycobacterium tuberculosis* culture and ribonucleic acid (RNA) study, as well as pulmonary pathology.

Case Report

A 67-year-old healthy man presented with chronic cough for 3 months. Physical examination was negative except for bronchial sounds in the right middle lobe (RML) field and coarse crackles in the left upper lung (LUL) field. The posteroanterior chest radiograph showed a pulmonary mass lesion in the RML and another mass lesion with a cavity in the LUL (Figure 1). Chest computed tomography (CT) also revealed a 4.5 x 4.6 cm lung mass in the RML with hilar lymph node enlargement, adjacent to the right-side pericardium (Figure 2A). Another 2.2 x 3.9 cm cavity lung mass with several surrounding fluffy nodules in the LUL was also noted, implying a feature of pulmonary tuberculosis (Figure 2B). Acid-fast stains for sputum were checked and the results were negative. Lung cancer was highly suspected, although left-side pulmonary tubercu-



Fig. 1. Chest posteroanterior radiograph showing a well-defined lung mass in the right middle lobe without rib destruction extending to the right hilum, and another cavitary lung mass in the left upper lobe.

losis could not be completely ruled out; therefore, a bronchoscopic examination was arranged for pathologic and bacteriologic diagnoses. It was also important to determine the nature of both lung masses in the RML and LUL. If both lung masses were malignant, the staging of lung cancer would be stage IV, as lung-to-lung metastases. If the LUL lung mass was a benign lesion, the staging of lung cancer would be dependent on the extent of local advancement.

Bronchoscopy with EBUS was performed with this patient. The ultrasonic pattern of the RML mass was heterogeneous with hyperechoic dots. No concentric circles were found and the margin was continuously hyperechoic (Figure 3A). The ultrasonic pattern of the LUL mass was homogeneous with a discontinuous hyperechoic margin. The ultrasonic image also presented air density (cavities) and concentric circles. No vessels or bronchiole presentation was found

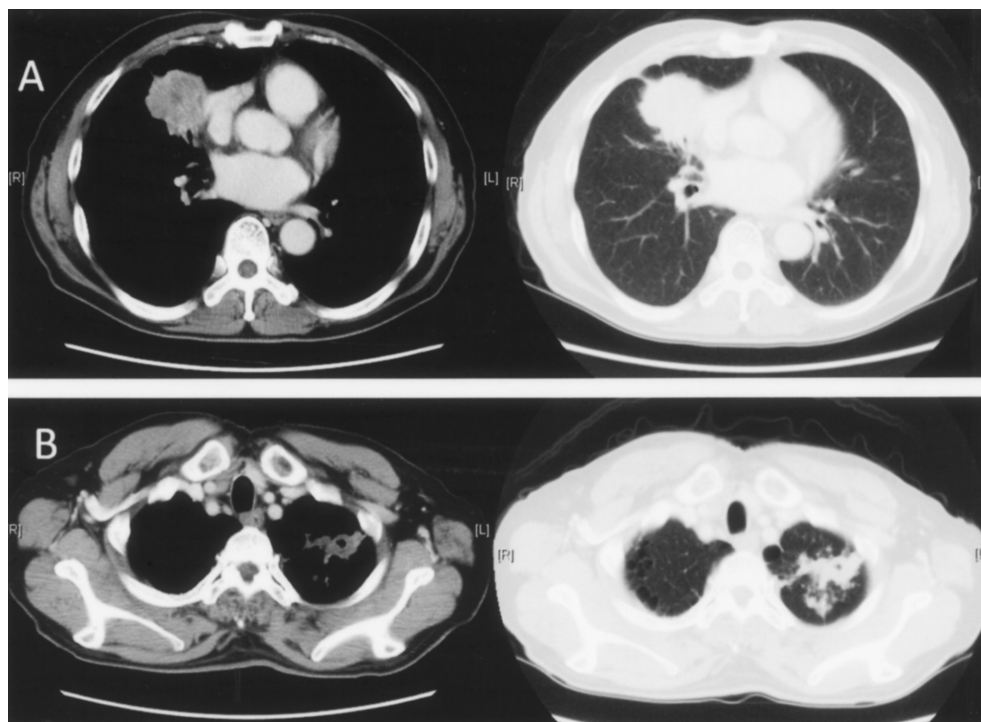


Fig. 2. Computed tomography. (A) A 4.5 x 4.6 cm lobulated lung mass in the right middle lobe, adjacent to the pericardium; (B) A cavitary lung mass in the left upper lobe had a variable thick wall and irregular shape. There were some fluffy nodules around the lung mass.

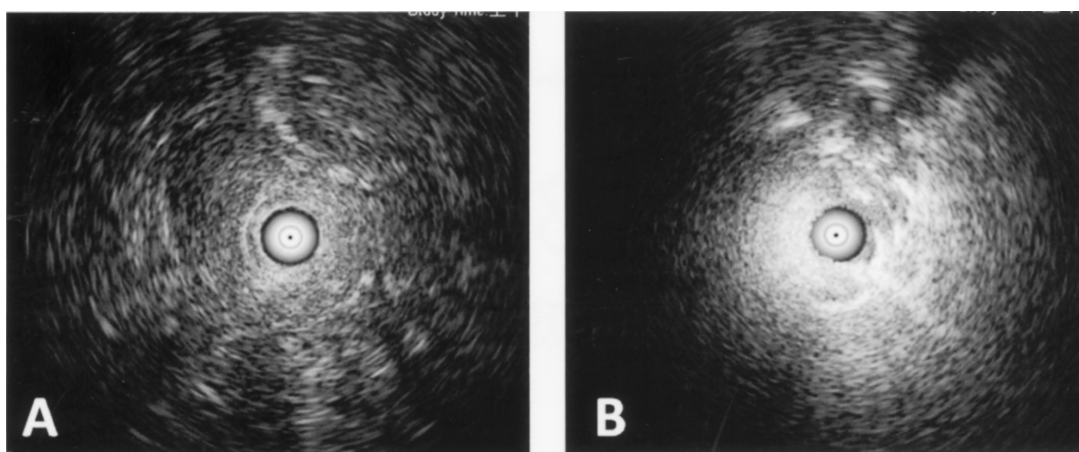


Fig. 3. Endobronchial ultrasonography. (A) Picture from the right middle lung mass showing heterogeneity, without concentric circles and with a continuous hyperechoic margin; (B) Picture of the left upper lung mass showing homogeneity, with hyperechoic dots, a discontinuous hyperechoic margin, and concentric circles.

(Figure 3B). Under EBUS guidance, transbronchial lung biopsy (TBB) via the RML and LUL were performed and bronchoalveolar lavage was

collected from the LUL for TB culture and TB RNA study. The pathologic finding of the RML mass was adenocarcinoma (Figure 4A), while the

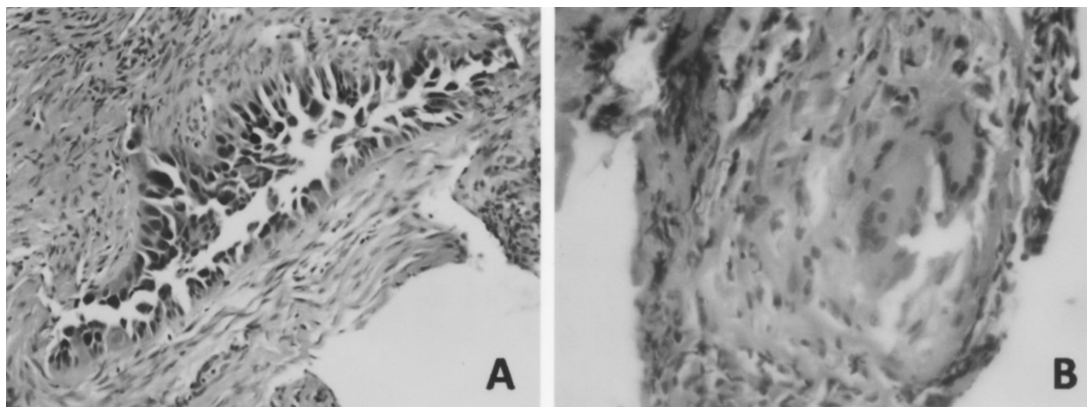


Fig. 4. (A) Adenocarcinoma characterized by infiltrating glands with nuclear hyperchromatism and pleomorphism. (hematoxylin and eosin, X 100 original magnification); (B) A small epithelioid granuloma with Langhan's giant cells. (hematoxylin and eosin, X 200 original magnification)

pathologic report of the LUL mass was epithelioid granuloma with Langhan's giant cell infiltration (Figure 4B). The TB RNA and tuberculin skin test (Mantoux test) results were both positive. The patient began treatment with isoniazid, rifampin, pyrazinamide, and ethambutol at that time. The sputum cultures also later confirmed *Mycobacterium tuberculosis* infection.

Thoracotomy was performed for further staging of the lung cancer. The RML adenocarcinoma invading the right upper lobe and right hilum directly was found and was tightly adherent to the pericardium. Surgical findings demonstrated T4N1, and no distant metastasis was found in further studies. Therefore, this patient was classified as stage IIIB adenocarcinoma, and has been treated with chemotherapy until now.

Discussion

Our report demonstrated that EBUS is a useful tool for localizing peripheral lung lesions and for differentiating benign from malignant abnormalities. Lung cancer is the leading cause of cancer-related deaths worldwide [10], including Taiwan [11-12]. Furthermore, the incidence

of pulmonary tuberculosis (TB) has risen recently owing to the occurrence of the AIDS epidemic and multi-drug resistant tuberculosis [13]. Moreover, pulmonary TB remains an endemic disease in Taiwan and studies have proved that lung cancer and active pulmonary mycobacteriosis are not uncommonly intermingled in the same lobe of the lung, with pictures of variable mixtures [14], so it is critically important for physicians to diagnose lung nodules carefully. The pathogenesis of the coexistence of the 2 diseases is under investigation. According to the study by Tamura *et al.* [15], there were 2 types of macroscopic images: (1) type A, in which the foci of lung cancer and tuberculosis were separate originally, progressed mutually, and became adjoined finally, and (2) type B, in which the foci of mycobacteriosis existed within or on the edge of the foci of the lung cancer. It has been suggested that cancer and mycobacteriosis are often adjoined under the conditions of preexisting lung disease in nontuberculous mycobacteriosis, whereas in pulmonary TB, the wall of the encapsulated caseous nodules is destroyed by cancer invasion, and therefore the tuberculous nodules were reactivated [15]. Studies have shown that the

increased occurrence of lung cancer in active tuberculosis patients may be connected with immunodepression caused by chronic TB infection [16]. In contrast, chronic pulmonary inflammation may also induce lung cancer. The production of reactive oxygen species (ROS), the activation of growth factors, and the altered signaling transduction processes, which are responsive to tissue damage and repair, have been considered as inducing factors for lung cancer formation [17]. The alteration of cellular immunity induced by chronic infection may facilitate the escape of transforming tumor cells from recognition and elimination by the immune system [18].

Accurate diagnosis of peripheral pulmonary lesions has relied on fluoroscopic guidance and transbronchial biopsy [19]. But, with the development of small-caliber miniature ultrasound probes and in combination with bronchoscopy, EBUS has been used to diagnose pulmonary and mediastinal lesions and to visualize the internal features of the pulmonary abnormalities [20]. Using EBUS guidance, the diagnostic yield of transbronchial lung biopsy of peripheral lung lesions by bronchoscopy has significantly improved, without any increase in the complication rate [3]. Additionally, EBUS-guided transbronchial biopsy has averted the need for surgical procedures [21].

Kurimoto *et al.* described a 3-type/6-subtype classification system to distinguish between benign and malignant diseases of peripheral pulmonary lesions using EBUS based on the internal structure of the lesion, internal echoes, vascular and bronchial patency, and the morphology of the hyperechoic areas [9]. According to their definition, the pulmonary lesion can be classified as follows: Type I, a homogeneous pattern (Type Ia, with patent vessels and patent bronchioles; Type Ib, without vessels and bronchioles); Type

II, hyperechoic dots and a linear arc pattern (Type IIa, without vessels; Type IIb, with patent vessels); and Type III, a heterogeneous pattern (Type IIIa, with hyperechoic dots and short lines; Type IIIb, without hyperechoic dots and short lines) [9]. In Kurimoto's report, 23 of 25 type I lesions (92.0%) were benign; while 98 of 99 type II and III lesions (99.0%) were malignant. Moreover, all type IIIb lesions (22 of 22, 100.0%) were malignant. [9]

Kuo *et al.* have further simplified the classification, based on the histological features of lung cancer and neighboring lung tissue, into 3 characteristic features in favor of malignancy: 1) the continuous margin of lesions with adjacent lung tissue, 2) the presence of continuous hyperechoic lines within the lesions (the presence of linear, dotted or mottled hyperechoic densities on ultrasonograph, and 3) heterogeneous echogenicity of internal structures [8]. In this report, the endobronchial ultrasonograph of the RML mass of the patient was heterogeneous in echogenicity with hyperechoic dots and a continuous hyperechoic margin with adjacent structure, which favor a malignant lesion. In contrast, the echogenicity of the LUL mass was homogeneous, with hyperechoic dots (cavities with air density) and a discontinuous hyperechoic margin with the adjacent structure, and without hypoechoic vessels, which favor a benign lesion. The echogenic patterns of both masses were compatible with the final pathology, adenocarcinoma in the RML and TB granuloma in the LUL, respectively.

In conclusion, for a lung nodule or mass, physicians should carefully note the mixture of tuberculosis and lung cancer. EBUS is a useful tool to guide transbronchial biopsy and to facilitate the differential diagnosis between benign and malignant abnormalities.

Acknowledgments

The authors are grateful to Dr. Yu-Lun Lo, a visiting lecturer and scientist at the School of Medicine, Harvard University, MA, USA, for his suggestions and careful review of the manuscript.

References

1. Tamura A, Hebisawa A, Tanaka G, *et al.* Active pulmonary tuberculosis in patients with lung cancer. *Kekkaku* 1999; 74: 797-802.
2. de Gracia J, Bravo C, Miravittles M, *et al.* Diagnostic value of bronchoalveolar lavage in peripheral lung cancer. *Am Rev Respir Dis* 1993; 147: 649-52.
3. Yang MC, Liu WT, Wang CH, *et al.* Diagnostic value of endobronchial ultrasound-guided transbronchial lung biopsy in peripheral lung cancers. *J Formos Med Assoc* 2004; 103: 124-9.
4. Kurimoto N, Miyazawa T, Okimasa S, *et al.* Endobronchial ultrasonography using a guide sheath increases the ability to diagnose peripheral pulmonary lesions endoscopically. *Chest* 2004; 126: 959-65.
5. Herth FJ, Ernst A, and Becker HD. Endobronchial ultrasound-guided transbronchial lung biopsy in solitary pulmonary nodules and peripheral lesions. *Eur Respir J* 2002; 20: 972-4.
6. Chao TY, Lie CH, Chung YH, *et al.* Differentiating peripheral pulmonary lesions based on images of endobronchial ultrasonography. *Chest* 2006; 130: 1191-7.
7. Omori S, Takiguchi Y, Hiroshima K, *et al.* Peripheral pulmonary diseases: evaluation with endobronchial US initial experience. *Radiology* 2002; 224: 603-8.
8. Kuo CH, Lin SM, Chen HC, *et al.* Diagnosis of peripheral lung cancer with three echoic features via endobronchial ultrasonography. *Chest* 2007(*in press*).
9. Kurimoto N, Murayama M, Yoshioka S, *et al.* Analysis of the internal structure of peripheral pulmonary lesions using endobronchial ultrasonography. *Chest* 2002; 122: 1887-94.
10. Peto R, Chen ZM, and Boreham J. Tobacco—the growing epidemic. *Nat Med* 1999; 5: 15-7.
11. Ando M, Wakai K, Seki N, *et al.* Attributable and absolute risk of lung cancer death by smoking status: findings from the Japan Collaborative Cohort Study. *Int J Cancer* 2003; 105: 249-54.
12. Zhang H, and Cai B. The impact of tobacco on lung health in China. *Respirology* 2003; 8: 17-21.
13. Rubin SA. Tuberculosis and atypical mycobacterial infections in the 1990s. *Radiographics* 1997; 17: 1051-9.
14. Sakuraba M, Hiramata M, Hebisawa A, *et al.* Coexistent lung carcinoma and active pulmonary tuberculosis in the same lobe. *Ann Thorac Cardiovasc Surg* 2006; 12: 53-5.
15. Tamura A, Hebisawa A, Sagara Y, *et al.* Coexistence of lung cancer and active pulmonary mycobacteriosis. *Kekkaku* 2005; 80: 413-9.
16. Rybacka-Chabros B, Mandziuk S, Berger-Lukasiewicz A, *et al.* The coexistence of tuberculosis infection and lung cancer in patients treated in pulmonary department of Medical Academy in Lublin during last ten years (1990-2000). *Folia Histochem Cytobiol* 2001; 39 Suppl 2:73-4.
17. Ardies CM. Inflammation as cause for scar cancers of the lung. *Integr Cancer Ther* 2003; 2: 238-46.
18. Gabrilovich D, and Pisarev V. Tumor escape from immune response: mechanisms and targets of activity. *Curr Drug Targets* 2003; 4: 525-36.
19. Zavala DC. Diagnostic fiberoptic bronchoscopy: Techniques and results of biopsy in 600 patients. *Chest* 1975; 68: 12-9.
20. Hurter T, and Hanrath P. Endobronchial sonography in the diagnosis of pulmonary and mediastinal tumors. *Dtsch Med Wochenschr* 1990; 115: 1899-905.
21. Herth FJ, Eberhardt R, Becker HD, *et al.* Endobronchial ultrasound-guided transbronchial lung biopsy in fluoroscopically invisible solitary pulmonary nodules: a prospective trial. *Chest* 2006; 129: 147-50.

應用支氣管鏡超音波鑑診斷肺癌與肺結核 —病例報告與文獻回顧

王才郁 郭志熙 陳豪成 吳仁欽* 劉劍英

同時存在肺癌和肺結核在台灣並非不常見，所以對於臨床醫師而言，決定肺部腫瘤的本質對於診斷和治療是很重要的。只使用支氣管鏡來診斷周邊肺部異常病灶，診斷率是受限的。然而、使用支氣管內超音波能更準確的定位肺部周邊異常的病灶並且增加診斷率。而且支氣管鏡超音波的影像也能幫忙鑑別診斷惡性與良性的病灶。在一位同時具有肺癌以及肺結核的六十七歲男性，在不同的肺葉分別發現兩個肺部腫瘤。支氣管鏡超音波在右中葉的病灶發現的影像是非均勻並有連續性高回響的邊緣，而在左上葉的病灶則是高回響的影像點以及沒有連續性高回響的邊緣。這兩種型態分別代表著惡性與良性。病理檢驗與肺結核菌的培養分別證實診斷右中葉的肺癌以及左上葉的肺結核。我們回顧了肺癌和肺結核同時並存之致病因以及支氣管鏡超音波對於肺部周邊病灶的影像特徵與輔助診斷之相關文獻報告。(胸腔醫學 2008; 23: 66-72)

關鍵詞：支氣管鏡超音波，肺結核，肺癌